Journal of Materials Chemistry A

REVIEW

View Article Online
View Journal | View Issue

Cite this: J. Mater. Chem. A, 2022, 10, 6397

Enrichment of low concentration methane: an overview of ventilation air methane

Zhuxian Yang,*[a] Mian Zahid Hussain,[a] Pablo Marín,[b] Quanli Jia,[c] Nannan Wang,[d] Salvador Ordóñez,[b] Yanqiu Zhu[a] and Yongde Xia*[a]

Methane (CH_4) is the second most important greenhouse gas after carbon dioxide (CO_2), but its global warming potential is 21–28 times that of CO_2. Coal mining accounts for 9% of global CH_4 emissions, among which 60–70% is contributed by ventilation air methane (VAM). Currently the simplest way to reduce CH_4 emissions from ventilation air is to thermally oxidize it to CO_2; however the low and changeable CH_4 concentrations (0.1–1.5% CH_4) and the large volume of ventilation air make it a challenge since conventional technologies used for CH_4 separation/purification in natural gas (CH_4 concentration 55–98%) are not suitable for VAM enrichment. It is therefore highly desirable to concentrate VAM up to levels for further harnessing, as the utilization of VAM can not only reduce CH_4 emissions but also provide extra economic benefits to relevant industries. Herein, for the first time, we present a review on both unconventional technologies and materials for VAM enrichment. The feasibility of technologies including vortex tubes, mechanical towers, gas hydrates, membranes and adsorption-based processes has been discussed, with focus on adsorption-based processes. Given that the adsorbents used in adsorption-based processes are one of the key factors for gas enrichment performance, materials including zeolites, porous carbon materials and metal–organic frameworks for methane separation have been critically analyzed and overviewed, covering the summary of the textural

Received 12th October 2021
Accepted 11th February 2022

DOI: 10.1039/d1ta08804a

rsc.li/materials-a

[a]College of Engineering, Mathematics and Physical Sciences, University of Exeter, Exeter, EX4 4QF, UK. E-mail: z.yang@exeter.ac.uk; y.xia@exeter.ac.uk

[b]Catalysis, Reactors and Control Research Group (CRC), Department of Chemical and Environmental Engineering, University of Oviedo, Facultad de Química, Julián Clavería 8, 33006 Oviedo, Spain

[c]Henan Key Laboratory of High Temperature Functional Ceramics, Zhengzhou University, Zhengzhou, 450052, PR China

[d]Guangxi Institute for Fullerene Technology (GIFT), Key Laboratory of New Processing Technology for Nonferrous Metals and Materials, Ministry of Education, School of Resources, Environment and Materials, Guangxi University, Guangxi, 530004, China

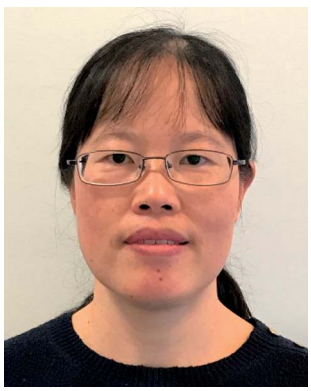

Zhuxian Yang received her BSc from East China Normal University in 1995 and her MSc from Fudan University, China in 1998. She earned her PhD in 2007 from the School of Chemistry at the University of Nottingham in the United Kingdom, working on the synthesis, characterization and application of micro/mesoporous carbon materials. She is now a Research Fellow in the College of Engineering, Mathematics and Physics Sciences, University of Exeter, working on the conversion of carbon dioxide to dimethyl carbonate. Her research interests include the applications of porous materials in gas storage and separation, as catalysts and electrocatalysts.

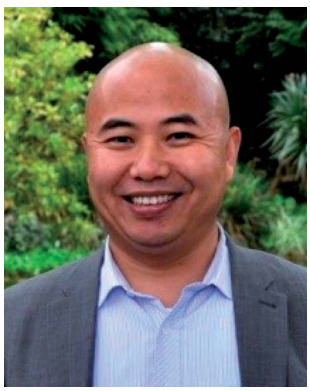

Yanqiu Zhu has been a Chair of Functional Materials at the University of Exeter since 2010. He obtained his BSc, MSc and PhD in China, in 1989, 1992 and 1996, respectively. He has research experience in China, Japan and the UK. He worked at the University of Sussex and University of Nottingham, prior to joining Exeter. His research covers a wide range of materials science and engineering, with special interest in functional nanomaterials and nanocomposites. He is an author/co-author of over 200 journal publications.

properties, CH_4 adsorption capacity, CH_4/N_2 equilibrium selectivity and CO_2/CH_4 equilibrium selectivity of these materials under ambient conditions and highlighting some new synthesis strategies to achieve high CH_4 adsorption capacity and CH_4/N_2 equilibrium selectivity. This review not only provides state-of-the-art technologies and materials for VAM enrichment (also applicable to other low grade CH_4), which will inspire further studies to better mitigate and utilize VAM and other low grade CH_4, but also supports the upcoming low-carbon economy.

1. Introduction

It is more urgent than ever to cut down on greenhouse emissions given that we are confronting frequent extreme weather events. As the second most important greenhouse gas after carbon dioxide (CO_2), methane (CH_4) possesses global warming potential (GWP) 21–28 times that of CO_2 for a 100 year time horizon.[1] CH_4 is released mainly from enteric fermentation (livestock), energy industry, landfills, wastewater treatment, rice cultivation, *etc.* The estimated global anthropogenic CH_4 emissions by the source in 2020 is 9390 million metric tons of CO_2 equivalent, of which 9% is contributed by coal mining. Fig. 1 shows the estimated global anthropogenic CH_4 emissions by sources.[2] The global CH_4 emissions from coal mining continue growing even with the declining coal production.[3]

Coal production releases CH_4 trapped in coal seams and surrounding strata, which can be categorized into three types of CH_4: CH_4 drained from the seam before mining (60–95% CH_4), CH_4 drained from worked areas of the mine (30–95% CH_4) and CH_4 diluted through ventilation fans (0.1–1.5% CH_4) while extracting coal.[4,5] Drained gas with CH_4 concentration more than 30% normally can be upgraded for pipeline quality gases or readily used by industries for heating or power generation.[6] The diluted CH_4 through ventilation fans is discharged to the atmosphere *via* mine exhausts and is called ventilation air methane (VAM). The VAM gas mixture is characterized by large volume (200–385 $m^3\ s^{-1}$), the majority being air (nitrogen ~79%, oxygen ~20%, carbon dioxide 0.13–0.19% and small amounts of other gases), low and changeable VAM concentration (0.1–1.5%), high relative humidity (70–100%) and high dust loading (0.13–4.47 mg m^{-3}).[4,7] VAM contributes about 60–70% of total CH_4 emissions from coal mining activities.[6,8] Therefore, the utilization of VAM can not only reduce greenhouse gas emissions, but also provide extra economic benefits to the mining industry.

The key challenges of VAM mitigation and utilization are the low and changeable CH_4 concentrations (0.1–1.5% CH_4), the large volume, the high relative humidity, and the high dust loading of ventilation air.[4] Currently the simplest way to reduce CH_4 emissions from ventilation air is to thermally oxidize it *via* the reaction $CH_4 + 2O_2 \rightarrow CO_2 + 2H_2O$.[9] In the oxidation processes, VAM is used as either an ancillary fuel or the principal fuel in lean-burn gas turbines, recuperative gas turbines, thermal flow reversal reactors (TFRRs) and catalytic flow reversal reactors (CFRRs).[8,10–12]

By converting CH_4 into CO_2, the effect of CH_4 on climate change can be significantly reduced given that the GWP of CH_4 is 21–28 times that of CO_2. In addition, the thermal energy produced from the CH_4 oxidation process can be readily utilized for domestic or industrial applications. Technologies for energy recovery are commercially available, but they are not very effective when the CH_4 concentration is less than 0.5%.[13] In addition, for lean-burn gas turbines, a CH_4 concentration of 0.8–2% (a minimum CH_4 concentration of 0.8%) is required for self-sustaining operation.[8,10,14] Therefore, it is highly desirable to concentrate VAM up to levels for further harnessing. If CH_4 can be concentrated to approximately 30% or higher, it can be used for conventional gas turbines without significant modifications to generate electricity.[8]

There have been excellent reviews on the emission sources and mitigation options for the major CH_4 sources,[6,8,15–17] in addition, the latest developments and opportunities in CH_4 mitigation technologies have been presented by Pratt *et al.* recently.[18] However, to the best of our knowledge, there has been no comprehensive analysis and overview on the enrichment and mitigation of VAM. Given that VAM contributes about 60–70% of total CH_4 emissions from coal mining activities,[6,8] it is of great importance to present a dedicated review on the enrichment of VAM, to discuss the current advance in technologies and materials for VAM enrichment and to inspire further studies in relevant areas, and consequently to better mitigate and utilize VAM, which will not only cut down on the VAM emission, but also provide extra economic benefits to the mining industry.

Herein, for the first time, we present a review to discuss and analyze the technologies and materials for VAM enrichment. Because the conventional technologies widely used for CH_4 separation/purification from natural gas (CH_4 concentration of 55–98%) are not suitable for VAM enrichment, we first discuss

Yongde Xia earned his PhD from Fudan University in 1999. After one year as a postdoctoral researcher at the Korea Advanced Institute of Science and Technology and another year at the University of Paris-Sud, France, he then moved to the UK and worked as a Research Fellow at the University of Nottingham. Followed by joining Exeter in 2010, he is now a Senior Lecturer in Functional Materials in the College of Engineering, Mathematics and Physics Sciences at the University of Exeter. His main research interests include novel porous materials for energy, electrochemical energy storage and conversion, photocatalysis and adsorption.

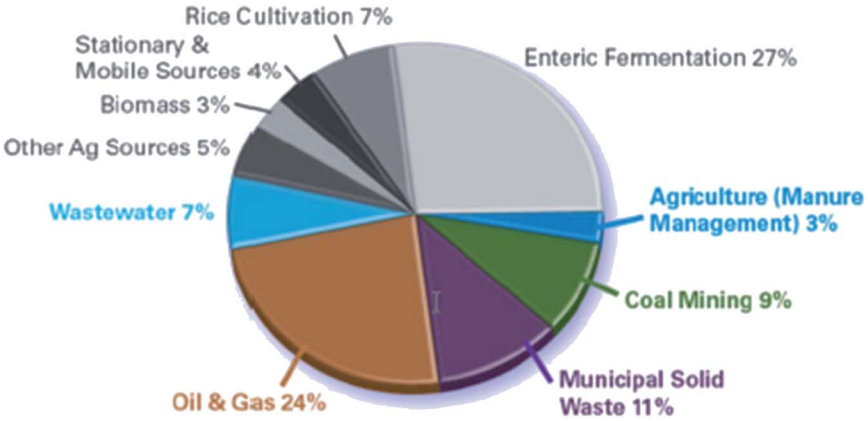

Fig. 1 Estimated global anthropogenic CH_4 emissions by sources. Adapted with permission.[2] Copyright 2020, Global Methane Initiative website.

the unconventional technologies including vortex tubes,[19–23] mechanical towers,[24,25] gas hydrates,[26–28] membranes[29,30] and adsorption based processes,[31–35] with focus on adsorption-based processes. Since the adsorbents used in adsorption-based processes are one of the key factors for gas separation/enrichment performance, we then discuss various materials including zeolites, porous carbon materials and metal–organic frameworks (MOFs) that are potentially useful as adsorbents for VAM and other low grade CH_4 enrichment, with focus on porous carbon materials and MOFs. Apart from the summary on the textural properties, CH_4 adsorption capacity, CH_4/N_2 equilibrium selectivity and CO_2/CH_4 equilibrium selectivity of these materials under ambient conditions, new synthesis strategies for materials with high CH_4 adsorption capacity and high CH_4/N_2 equilibrium selectivity have been highlighted. Finally, we draw conclusions and provide prospective research directions in this field.

2. Technologies for CH_4 separation from ventilation air

Generally, gas separation may involve one of the following mechanisms: phase creation by heat transfer to or from the mixture, absorption in a liquid solvent, adsorption on a solid adsorbent or permeation through a membrane. The differences in gas properties, such as the kinetic diameter, polarizability, quadrupole and dipole moments, could be harnessed for gas separation.[36] The key challenge to separate CH_4 from ventilation air is the similar chemical and physical properties of CH_4, CO_2 and N_2, as listed in Table 1.[37] Due to these similar properties, the adsorbents with high CH_4 uptake capacities also exhibit high CO_2 uptake capacities.[29,36] The significant difference in the polarizability between CH_4 and N_2 could be exploited to separate CH_4 from N_2, which has been demonstrated by some MOFs.[38–40]

Conventional technologies for natural gas (containing 55–98% CH_4) separation include cryogenic distillation to remove N_2 and higher hydrocarbons, dehydration by adsorption to remove H_2O, and gas sweetening by amine absorption to remove acidic gases (CO_2 and H_2S). Cryogenic distillation requires a gas–liquid phase change, which will add a significant energy cost. These processes become uneconomic or impractical when the CH_4 content is below about 40%. In the case of VAM where the CH_4 concentration varies in the range of 0.1–1.5%, it is highly desirable to separate or selectively adsorb CH_4 itself from the gas mixture (the majority is air), so as to concentrate or enrich CH_4 for further utilization.[41] In this section, we will first discuss the feasibility of unconventional technologies for CH_4 separation/enrichment from ventilation air.

Unconventional technologies that have been investigated for gas separation include vortex tubes,[19–23] mechanical towers,[24,25] gas hydrates,[26–28] membranes[29,30] and adsorption based separation.[31–35] The first three (vortex tubes, gas hydrates and mechanical towers) are technologies/concepts without commercial applications currently, but the last two (membrane separation and adsorption-based separation) have been used on a commercial scale for natural gas and other gas separation. We will discuss the feasibility of these technologies in the application of VAM enrichment in the following part.

2.1. Vortex tubes

A vortex tube, also known as a Ranque–Hilsch vortex tube, is a simple mechanical device. It separates a compressed fluid that

Table 1 Properties of CH_4, N_2 and CO_2 gases. Reproduced with permission.[37] Copyright 1994, Elsevier

Gas	Molecular weight (g mol^{-1})	Kinetic diameter (nm)	Polarizability ($\times 10^{-25}$ cm^3)	Dipole moment ($\times 10^{18}$ esu cm)	Quadrupole moment ($\times 10^{-26}$ esu cm^2)
CH_4	16	0.38	26.0	0.00	0.00
N_2	28	0.364	17.6	0.00	1.52
CO_2	44	0.33	26.5	0.00	4.30

tangentially enters the vortex chamber through inlet nozzles into two streams, the cold one at one end of the tube and the hot one at the other end. It was hypothesized that a stream of a compressed gas mixture flew into the vortex tube could be separated into individual gas streams based on the differential centrifugal forces acting on them.[19] Linderstrom-Lang experimentally studied the gas separation of three gas mixtures (O_2/N_2, O_2/CO_2, and O_2/He) in a vortex tube in detail. They found that gas separation was created by centrifugation, supporting the centrifugation hypothesis.[20] Gas separation by using a vortex tube is relatively less investigated.[19–23]

Kulkarni *et al.* studied the separation of a gas mixture of CH_4 and N_2 with a vortex tube to verify if gas separation occurs. Fig. 2 shows the schematic experimental setup. The two gases were mixed before passing through the vortex tube. Gas samples at the exits of the vortex tube were collected in gas sampling bags and were injected into a gas chromatograph for analysis. The two parameters including the inlet pressure and cold flow fraction (the ratio of mass of gases exiting the cold exit to the mass of gases entering the vortex tube) were studied. The results showed that gas separation took place in the vortex tube as evidenced by the CH_4 concentration at the cold and hot ends. Moreover, the experimental values and the calculated ones of gas separation were comparable. The inlet pressure was identified to be the most dominant factor affecting the separative power of a vortex tube of fixed geometry, and the higher the inlet pressure, the higher the separative power of the vortex tube.[19]

The advantage of a vortex tube is that it has no moving parts and does not break or wear, so it requires little maintenance. However, this technique does demand the inlet gas stream to be pressurized (165–248 kPa was used in the above study).[19] Given that the volume of ventilation air is huge, pressurizing it is a big issue. Further feasibility studies on CH_4 separation/enrichment from ventilation air *via* a vortex tube are very much needed.

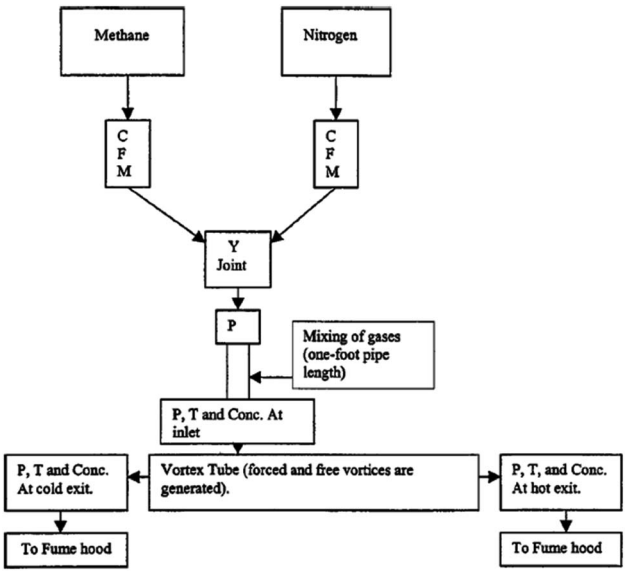

Fig. 2 Schematic experimental setup for the separation of a gas mixture of CH_4 and N_2 with a vortex tube. Adapted with permission.[19] Copyright 2002, American Society of Civil Engineers.

2.2. Mechanical towers

Wang *et al.* designed a mechanical tower for the enrichment of VAM by using CH_4 buoyancy under free diffusion conditions (namely, the gas mixture moves freely under the force of gravity) based on the fact that the density of CH_4 is lower than that of air.[24] The enrichment characteristics of segregated (CH_4 and N_2 enter the system separately) and non-segregated (CH_4 and N_2 are pre-mixed before entering the system) mixtures under free diffusion conditions were studied. For a CH_4/N_2 mixture with 0.5% CH_4, a CH_4 concentration of 0.54% was monitored for the non-segregated mixture, which is not promising.

Recently Wang *et al.* carried out a follow up study using a similar mechanical tower for the VAM (0.5% CH_4) enrichment, under free diffusion conditions and weak eddy conditions, respectively. For a non-segregated mixture, under weak eddy field conditions, the maximum CH_4 concentration is 0.54% (0.55%) in the top (middle) tower.[25] This enrichment from 0.5% to 0.55% is far from enough for lean-burn gas turbines, which require a minimum CH_4 concentration of 0.8% for self-sustaining operation.[8,10,14] Since this technique is based on the difference in the density of the gases to be separated, significant improvement in the CH_4 enrichment performance with this technique seems difficult.

2.3. Gas hydrates

Gas hydrates (clathrate hydrates) are crystalline solid structures formed *via* the inclusion of gas molecules (such as CH_4, N_2, O_2, CO_2, H_2, *etc.*) into cavities of the frame built from hydrogen-bound water molecules without forming a chemical bond between the gas molecules and the water molecules. Generally, low temperature and high pressure are required for the formation of gas hydrates.[42] However, the use of thermodynamic promoters, such as tetra-*n*-butyl ammonium bromide (TBAB), tetra-*n*-butyl ammonium chloride (TBAC), tetrabutyl phosphonium bromide (TBPB) *etc.*, has been reported to be able to reduce the hydrate formation pressure.[43–45]

CH_4 separation from coal mine methane (CMM) *via* hydrate formation has been extensively investigated,[44,46,47] but only a few studies on CH_4 separation from ventilation air *via* hydrate formation have been reported. In particular, Adamova *et al.* theoretically calculated the hydrate formation of VAM (0.5% CH_4, 75% N_2, and 24.5% O_2) in the temperature range of 258 to 273 K and the pressure range of 0.1 to 35.5 MPa.[26] At 273 K and 17.96 MPa, CH_4 concentration in the gas clathrate is 1.9%, nearly 4 times that in the gas phase (0.5%). Based on this theoretical study and the formation of methane hydrate under milder conditions (282.7–291.5 K and 0.15–5.10 MPa) achieved with the addition of TBPB,[45] Du *et al.* investigated phase equilibrium conditions for gas hydrates formed from simulated mine ventilation air in the presence of TBPB,[27] tri-*n*-butyl phosphine oxide (TBPO) or TBAB.[28] With 37.1 wt% TBPB, at 278 K and 4 MPa, CH_4 was enriched from 0.5% to 1.75% in the hydrate phase,[27] and with an addition of 5 wt% TBPO, approximately 3-fold CH_4 enrichment could be achieved in the hydrate phase.[28] They also proposed the concept of a hydrate-based CH_4 concentrator shown in Fig. 3, in which with 5 wt% TBPO, at 281

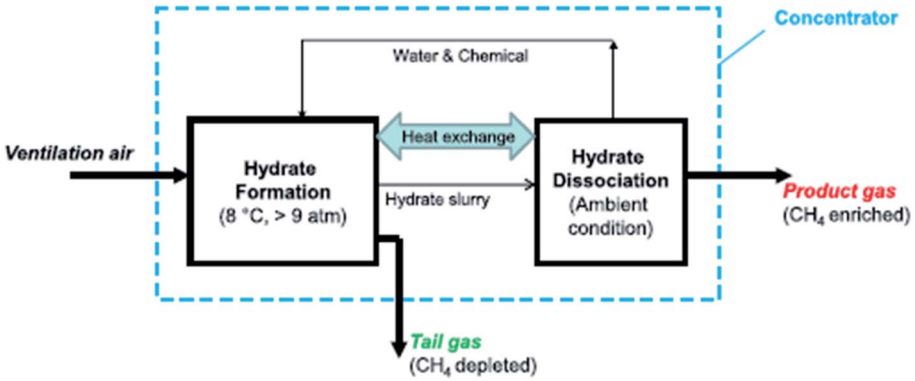

Fig. 3 Conceptual diagram of CH_4 enrichment *via* hydrate crystallization. The product gas released from hydrate decomposition can be fed to lean-burn turbines. Adapted with permission.[28] Copyright 2015, Elsevier.

K and pressure higher than 0.91 MPa, CH_4 could be enriched to a level meeting the requirements of lean-burn CH_4 utilization technologies.

Although the results of CH_4 separation from coal mine methane *via* hydrate formation are promising, the conditions (281 K and >0.91 MPa) for the formation of VAM hydrate are still a concern, because it would be a great challenge to cool and pressurize a large volume of ventilation air. Further studies on the energy cost and feasibility of VAM enrichment *via* a gas hydrate are urgently needed. Breakthroughs in the improvement of VAM hydrate formation conditions could make this method viable for practical application.

2.4. Membrane separation

Gas separation using membranes can offer the advantages of lower cost and smaller equipment size, lower energy consumption and ease of operation compared to conventional processes.[48] The usage of membranes has been widely employed for natural gas separation in industry for the removal of acidic gases, such as CO_2 and H_2S.[29,30] However, currently, membranes are not suitable for separating low concentration CH_4 from ventilation air because of the high costs of initial capital investment and membrane maintenance or replacement due to fouling.[13] Advances to make membrane separation systems commercially viable for VAM are highly demanded.[49]

2.5. Adsorption based processes

2.5.1. Basics of adsorption-based separation. Adsorption is a physical phenomenon in which molecules of a gas, vapor, or liquid become trapped within the nanosized pores of a solid material, which is called the adsorbent, and the trapped material is termed the adsorbate. The reverse of the adsorption process is called desorption. Different molecules interact with the adsorbents differently, which can be harnessed for separation. There are two types of separation mechanisms: equilibrium separation and kinetic separation, with the first one being more common and widely employed. In equilibrium separation, the adsorbent preferably adsorbs one type of molecule over others in the gas mixture, which depends either on the molecular size or kinetic diameter or affinity.[50–54] In kinetic separation, the adsorption rate of one component is faster than that of others in the gas mixture, which is very useful in the cases when the equilibrium uptakes of components are similar or when the size of the adsorbent pore is close to the size of the molecules to be separated.[29,55,56]

Accordingly, there are two types of selectivity, equilibrium selectivity and kinetic selectivity. Equilibrium selectivity (or thermodynamic selectivity) depends on the difference in adsorption at equilibrium, and kinetic selectivity depends on the difference in adsorption rates.

The equilibrium selectivity for a binary gas mixture of components i and j is defined as:

$$\alpha_{i/j} = \frac{x_i/x_j}{y_i/y_j} \quad (1)$$

where x_i and x_j are the mole fractions of components i and j in the adsorbed phase, and y_i and y_j are the mole fractions in the gas phase, respectively; the equilibrium selectivity can be calculated from adsorption data measured with pure component gases using an equilibrium thermodynamic model, such as ideal adsorption solution theory (IAST) or by computer modelling.[29,41,57] The value in eqn (1) changes depending on the mole fractions of components. Values greater than unity mean that component i is more strongly adsorbed than component j.

The equilibrium selectivity for a binary gas mixture of components i and j can be estimated by using eqn (2). The value in eqn (2) is a constant and only valid at a very low gas pressure and low adsorption loading on the adsorbent.[58]

$$\alpha_{i/j} \approx \frac{K_i}{K_j} \approx \frac{q_{mi} b_i}{q_{mj} b_j} \quad (2)$$

where K_i and K_j are Henry's law constants of components i and j, respectively; q_{mi}, b_i, q_{mj} and b_j are the Langmuir equation constants for components i and j, respectively.[29,41,58]

In a kinetically controlled separation process, both the kinetic and equilibrium effects determine the actual kinetic selectivity, which is given by the following equation in the linear range of the isotherms:[59,60]

$$S_K = \frac{K_{Hi}}{K_{Hj}}\sqrt{\frac{k_{\mu i}}{k_{\mu j}}} \quad (3)$$

where K_{Hi} and K_{Hj} are Henry's law constants of components i and j, and $k_{\mu i}$ and $k_{\mu j}$ are the overall mass-transfer coefficients of components i and j.

2.5.2. Adsorption-based separation processes. Typically, two types of adsorption-based separation processes have been studied for VAM enrichment: the fluid bed concentrator and the swing mode process that includes both pressure swing adsorption and temperature swing adsorption.

Fluid bed concentrators, widely used for volatile organic compounds, were proposed to concentrate CH_4 of very dilute VAM flows up to levels that might be beneficial as a fuel in a gas turbine, reciprocating engine, or support oxidation in a TFRR or CFRR.[61] The concentration principle is as follows: the bed concentrator consists of a series of perforated plates or trays supporting an adsorbent medium (*e.g.*, activated carbon beads). The VAM stream enters from the bottom of the concentrator and passes upward through the trays where it fluidizes the adsorbent medium to enhance the capture of CH_4. The CH_4 saturated adsorbent drops to the bottom of the concentrator, where it can be discharged to the storage vessel and then the desorber. The adsorbent is regenerated by increasing the temperature to release the adsorbed CH_4 into a stream of a lower flow rate and higher CH_4 concentration.[61] However, experimental results on a fluidized bed concentrator using simulated ventilation air with 0.5% CH_4 from Environmental C & C, Inc. in 2003 were not promising, and the trials were stopped.[8,61,62] It is worth mentioning that a lot of new and advanced adsorbents with high CH_4 adsorption capacities (up to 2.90 mmol g^{-1}) and high CH_4/N_2 selectivity (up to 12.5) have been prepared and studied since the trial.[38,63–71] Studies on the performance of concentrators with these newly developed adsorbents are highly desirable, which could lead to high performance and cost-effective concentrators.

In swing mode adsorption processes, at least two columns packed with adsorbents are required to carry out the separation process. The feed gas mixture passes through the first column, and the adsorbent selectively adsorbs one of the components till it is saturated. Then, the feed gas mixture is directed to the second column. Meanwhile, the first column is regenerated by desorbing the adsorbed component. When the second column is saturated, the feed gas mixture is directed toward the first column and the second column is regenerated.[29] In practice, multiple columns are employed in a swing-mode to make the process continuous and additional steps are added to maximize the productivity and reduce the energy consumption.[72] The adsorbed component is desorbed from the adsorbent in the regeneration process, which results in the enrichment of the adsorbed component. When the adsorbent is regenerated by desorption at a lower pressure than that used for the adsorption phase of the cycle, the process is termed pressure swing adsorption (PSA).[73] In the case of regeneration that takes place under vacuum, it is called vacuum pressure swing adsorption (VPSA) or vacuum swing adsorption (VSA).[74,75] When the adsorbent is regenerated by desorption at a higher temperature than that used for the adsorption phase of the cycle, it is called temperature swing adsorption (TSA).[76] Normally the feed gas is pressurized in the adsorption step, but in the case of VAM enrichment, given the large volume of the ventilation air flow, it would not be practical to pressurize the feed gas flow. Therefore, the operating pressure close to atmospheric pressure is preferred.[77]

Due to their low operational costs, high separation efficiency and flexibility compared to mature separation technologies, such as absorption and distillation, swing mode separation processes are widely used for natural gas separation and purification, the production of hydrogen, the separation of O_2 and N_2 from air, *etc.*[33] Recently, these processes have been extensively studied for the enrichment of low-grade CH_4 gas[78–80] and VAM[7,77,81–87] too. VAM enrichment has been investigated by several research groups, including University of Science and Technology Beijing,[81–84] Dalian University of Technology,[85] East China University of Science and Technology,[88] and Commonwealth Scientific and Industrial Research Organization (CSIRO).[7,77,86]

2.5.2.1. VPSA process. Early studies on VAM enrichment were carried out *via* the VPSA process.[81,82,85] For example, Liu *et al.* used coconut shell-based activated carbon as an adsorbent *via* the VPSA process at an adsorption pressure of 150 to 250 kPa, and the CH_4 concentration was improved from 0.3% to 0.73%.[87] Although the enriched VAM concentration was still below 1% in these early reports, it triggered further investigations in VAM enrichment *via* PSA processes. Later Quyang *et al.* studied VAM enrichment using a coconut shell-based activated carbon adsorbent (CH_4/N_2 selectivity of 6.18) *via* the VPSA process with a feed gas of 0.42% CH_4 and 99.58% N_2.[85] The concentration of CH_4 was enriched from 0.42% to 1.09%, which can satisfy the requirements of flow-reversal reactors or lean-burn combustion turbines to generate power.

Based on their early study,[87] Yang *et al.* recently carried out the VAM enrichment *via* a three-bed VPSA process unit which was equipped with a new vacuum exhaust step for the VPSA process.[84] The coconut shell-based active carbon with an equilibrium CH_4/N_2 selectivity of 5 was used as the adsorbent. On a lab scale, the VAM was enriched from 0.2% to 0.4% and 0.69% as the vacuum exhaust ratio increased from 0 to 3.1, respectively. Moreover, a pilot-scale test system has been built at Julong Mine, Jizhong Energy Handan Mig., Handan, China.[84] It uses a two-stage three-bed separation unit which can handle a flow rate of 500 m^3 h^{-1}. As shown in Fig. 4, the feed gas is compressed with a Roots blower (P1) and transferred to the adsorption bed of the first stage–stage separation unit. The CH_4-rich gas is vacuumed with a vacuum pump (VP1) and transferred to the second separation unit with a Roots blower (P2). The product is collected from the vacuum pump (VP2). The VAM was enriched from 0.2% to over 1.2% in this system, which is well above the minimum CH_4 concentration of 0.8% required for self-sustaining operation of lean-burn gas turbines,[8,10,14] making it promising for VAM enrichment. Further studies are expected to evaluate the cost, efficiency, *etc.* for commercial possibility.

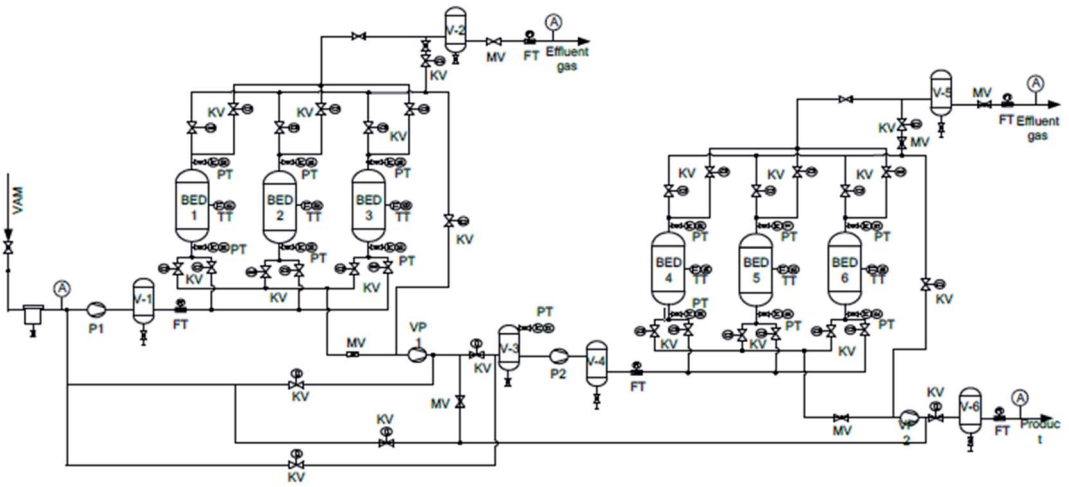

Fig. 4 Process diagram for the pilot plant. BED-adsorber; PT-pressure transmitter; TT-temperature transmitter; V-gas buffer; KV-pneumatic valve; FT-flowmeter; MV-gas-manual control valve; P1/P2-pump; VP1/VP2-vacuum pump; A-methane sensor.[84]

2.5.2.2. Vacuum swing (VS) followed by a temperature and vacuum swing adsorption (TVSA) process. Bae *et al.* developed a prototype VAM capture unit with a honeycomb monolithic carbon fiber composite (HMCFC) adsorbent and employed it in a large-scale test for VAM capture under various conditions in 2014.[5,77] In the regeneration stage, a new vacuum and temperature swing process is employed to desorb CH_4 from the adsorbent, involving initial VS followed by TVSA. The initial VS was found to be vital for the final CH_4 concentration. A VAM of less than 1% can be enriched by 5 or 11 times by one-step adsorption, and a CH_4 concentration of more than 25% can be achieved by two-step adsorption, as shown in Fig. 5. A VAM of less than 5% obtained from the one-step adsorption can be utilized as a principal fuel for lean burn turbines.

Based on the above study,[77] Bae *et al.* built up a two-stage prototype VAM enrichment unit with VTVSA in accordance with relevant Australian Standards and local mine site regulations. The enrichment of simulated ventilation air from 0.30%, 0.60%, and 0.98% CH_4 up to 19.28%, 24.24%, and 36.92% CH_4, respectively was demonstrated, avoiding the explosion range of 5–15% CH_4.[86] Very recently they have successfully carried out site trials of a two-stage VTVSA process using carbon fiber composites for VAM enrichment at an Australian coal mine.[7]

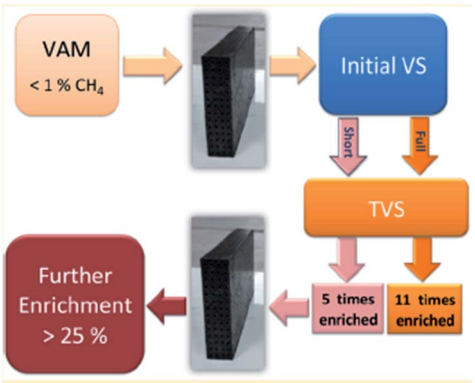

Fig. 5 Enrichment of simulated VAM with monolithic carbon fiber composites (MCFCs) by vacuum swing (VS) followed by combined temperature and vacuum swing adsorption (TVSA). Adapted with permission.[77] Copyright 2014, American Chemical Society.

The schematic diagram of the prototype VAM enrichment unit is shown in Fig. 6. About 22–60 L min^{-1} VAM from the outlet of an oxidation unit was fed to the prototype unit by using a blower with a variable speed drive, until CH_4 was detected in the exhaust stream of the first column. Then the first column was vacuumed until a predetermined pressure was reached. The HMCFC in the first column was then heated up to 383 K by circulating a heated thermal fluid (about 20 L min^{-1}), followed by vacuuming to desorb gas out of the column. The desorbed gas stream was fed to the second column. The hot thermal fluid in the first column was drained and cooled down to ambient temperature for the next test. These processes were repeated until the second column was saturated, which has undergone the same regeneration processes to produce the final product. The inlet VAM was enriched from 0.54–0.73% to 4.34–4.94% after the first stage and 27.62–35.89% after the second stage.[7] As mentioned by the authors, these VTVSA processes were scalable and portable to cope with changes in mine site operation and specifications, but the involvement of the energy intensive step of the temperature swing adsorption (TSA) process is an issue for practical applications. In this regard, the VPSA with CO_2 displacement process (VPSA-CO_2DIS) (discussed below) could be a solution to tackle this energy consultation issue.

2.5.2.3. VPSA with CO_2 displacement process (VPSA-CO_2DIS). Compared to CH_4, CO_2 is more strongly adsorbed by activated carbon, so in the VPSA-CO_2DIS process, after the column has adsorbed CH_4, the feed gas is switched to CO_2 and the adsorbed CH_4 is displaced and pushed out of the column by CO_2.[89] In 2011, Liu *et al.* studied the VPSA-CO_2DIS process with activated carbon as the adsorbent for coal bed CH_4 enrichment (CH_4/N_2 mixture of 17% CH_4). The results demonstrated a CH_4 enrichment from 17% up to 90% with CH_4 recovery higher than 98%.[89]

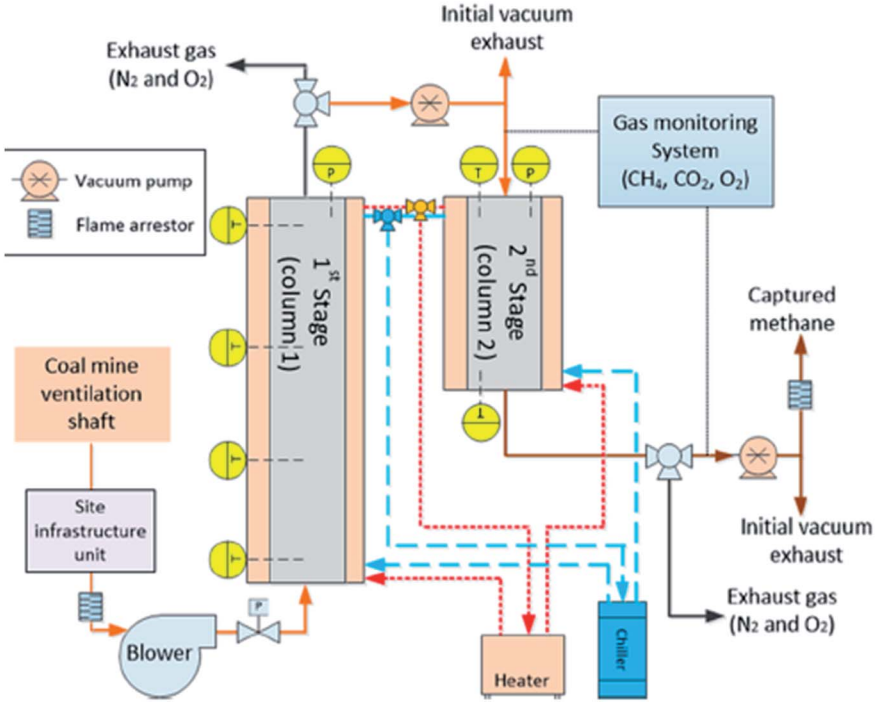

Fig. 6 Schematic diagram of the prototype VAM enrichment unit equipped with two-stage adsorption processes and installed at an Australian coal mine site. Adapted with permission.[7] Copyright 2020, American Chemical Society.

Based on this study, Yang *et al.* investigated the VPSA-CO_2DIS process with activated carbon beads as the adsorbent for the enrichment of VAM in 2016.[88] CH_4 enrichment from 1% to 53.5% was achieved, demonstrating that the VPSA-CO_2DIS process is promising for VAM enrichment. More studies on the cost, efficiency, scalability, *etc.* of the VPSA-CO_2DIS process for real VAM enrichment are highly demanded.

2.6. Summary on technologies for VAM enrichment

Among various technologies investigated for VAM enrichment, pressure swing adsorption (PSA)-based process has been the most studied and the most promising technology for VAM enrichment. Specifically, a pilot-scale study with the VPSA process and a site trial with the VTVSA process for VAM enrichment have been carried out by two research groups, respectively. Nevertheless, further studies on the cost, efficiency, scalability, *etc.*, are needed. Meanwhile, as discussed in the following part, many adsorbents with high CH_4 adsorption capacities (up to 2.90 mmol g^{-1}) and high CH_4/N_2 selectivity (up to 12.5) have been reported recently.[38,63–71] The use of some of these highly efficient adsorbents in PSA and/or TSA processes is expected to lead to improved VAM enrichment performance.

3. Materials for selective adsorption of CH_4 from CH_4–N_2 mixtures

The performance of PSA and TSA units for the enrichment of VAM is mainly determined by the adsorbents employed for the separation process, though the engineering of PSA and TSA units is also very important.[90] Adsorbents with simultaneously high CH_4/N_2 selectivity and high CH_4 adsorption capacity are preferred, as the former can reduce the number of cycles for the treatment of an input stream to reach a desired CH_4 concentration and the latter may lower the overall cost.[70] Therefore, information on the adsorption equilibrium and kinetic data of adsorbents is essential for the design of adsorption columns.[59,91]

Due to their porous nature, zeolites, carbon materials and metal–organic frameworks (MOFs) have been extensively studied as adsorbents for gas storage and separation.[29,36,92–96] For natural gas purification, studies have been devoted to the separation of N_2 and CO_2 from CH_4, in which case CH_4 is the major component and N_2 and CO_2 are impurities, so adsorbents with high N_2 or CO_2 adsorption capacities and high N_2/CH_4 selectivity or CO_2/CH_4 selectivity are preferred. Excellent reviews on natural gas separation/purification and related adsorbents can be found in the literature.[29,36,72]

In the case of VAM (and other low concentration CH_4) enrichment, the above adsorbents are naturally good candidates. However, adsorbents with high CH_4 adsorption capacity and high CH_4/N_2 selectivity are prerequisites given the low concentration of CH_4 (0.1–1.5%) in ventilation air and the large volume of ventilation air. It has been demonstrated that the CH_4 uptake amount is almost linearly related to the surface area of the adsorbent;[90,97] meanwhile, it has also been revealed that the optimum pore diameter for CH_4 adsorption is within the range of 0.7–1.0 nm.[98–100] Therefore, an adsorbent with a high surface area associated with an optimal pore size is the key prerequisite for high CH_4 adsorption capacity. Given that N_2

and CO_2 are present in ventilation air, low CO_2/CH_4 selectivity of the adsorbent is also important. In addition, due to the high relative humidity (70–100%) of ventilation air, the effect of water on the performance of the adsorbents also needs to be taken into account. Therefore, in the following part, we discuss the textural properties, CH_4 adsorption capacity, CH_4/N_2 equilibrium selectivity and CO_2/CH_4 equilibrium selectivity of these materials under ambient conditions unless otherwise specified, the effect of water on the adsorbents, and the advantages and disadvantages of the widely studied three types of adsorbents (zeolites, carbon materials and MOFs). In addition, we highlight new synthesis strategies to achieve high CH_4 adsorption capacity and high CH_4/N_2 equilibrium selectivity, including the combination of the advantages of zeolites and MOFs, or the advantages of carbon and MOFs, heteroatom (N or S) doping, and the surface property modification for porous carbons, the creation of coordinatively unsaturated metal centers for MOFs and the pore wall environment control of MOFs. It is worth noting that materials with relatively lower CH_4 adsorption capacity or lower CH_4/N_2 selectivity (compared to those listed in the tables) are excluded from the tables; if several samples were studied in the same paper, only some of them are listed in the tables.

3.1. Zeolites

Zeolites are 3-dimensional aluminosilicate frameworks constituted by Si and Al tetrahedra linked through bridged oxygen atoms giving rise to a regular distribution of pores and cavities of molecular dimensions. In the case of VAM separation, due to the close kinetic diameters of CH_4 (0.38 nm) and N_2 (0.364 nm), it is extremely difficult to separate them by using the molecular sieving effect; therefore the separation of CH_4 from N_2 by using the adsorption equilibrium difference between CH_4 and N_2 would be a better choice. Consequently, zeolites with high CH_4 adsorption capacity and high CH_4/N_2 selectivity are required.

The polarizability, dipole and quadrupole moments of a gas determine the strength of the interaction between the gas and the zeolite surface. Due to their large dipole and quadrupole moments, H_2O and CO_2 are usually the strongest adsorbed species on hydrophilic zeolites.[101] Given that ventilation air is usually saturated with H_2O and contains CO_2, zeolites with high CH_4/CO_2 selectivity are preferred for the separation of CH_4 from ventilation air. Kim *et al.* studied the CH_4 capture effectiveness of two classes of materials by computer modelling, including liquid solvents and zeolites, for a low-quality natural gas and VAM, respectively. Among the 190 experimentally realized International Zeolite Association (IZA) structures and over 87 000 predicted crystallography open database (PCOD) structures, they found that zeolites ZON and FER with the largest adsorbed CH_4/CO_2 ratio and $K_H(CH_4)$ (Henry's constant) of 1.29 and 1.12 mol kg^{-1} kPa^{-1}, respectively, are excellent candidates for concentrating a dilute CH_4 stream into moderate concentration.[41]

Wu *et al.* introduced the subunits of ZIFs into zeolite Y and zeolite ZSM-5 for CH_4/N_2 separation, based on a theoretical study that the preferential adsorption sites for CH_4 on ZIF-8 are in specific regions close to the organic imidazolate. The results showed that the CH_4/N_2 selectivity of the zeolites was greatly improved to above 8 at 100 kPa and 298 K, which was higher than that of zeolites and even better than that of ZIFs.[102] However, the CH_4 adsorption capacity is low, only 0.11–0.27 mmol g^{-1}. Nevertheless, this strategy provides a way to combine the advantages of the low cost and mature synthesis technology of zeolites and the high CH_4/N_2 selectivity of MOFs, avoiding the complicated and high costs of synthesis processes of MOFs. Other combinations of zeolites and MOFs could result in both high CH_4/N_2 selectivity and high CH_4 adsorption capacity.

Table 2 summarizes the textural properties, CH_4 adsorption capacities, CH_4/N_2 selectivity and CO_2/CH_4 selectivity of zeolites under ambient conditions. As shown in Table 2, the CH_4/N_2 selectivity of commercial zeolites 5A and 13X is less than 3.2 and the CH_4 adsorption capacities are less than 0.82 mmol g^{-1}.[50,58,103,104] The majority of zeolites in Table 2 show CH_4 adsorption capacities below 1 mmol g^{-1}, but ion-exchanged CHA (Li-CHA) shows a high CH_4 adsorption capacity of 1.47 mmol g^{-1} with a CH_4/N_2 selectivity of 4.7 and a CO_2/CH_4 selectivity of 32.[105] All the zeolites with available CO_2/CH_4 selectivity listed in Table 2 show that their CO_2/CH_4 selectivity is higher than their CH_4/N_2 selectivity, except for silicalite-I reported by Yang *et al.* with a CH_4/N_2 selectivity of 3.60 and a CO_2/CH_4 selectivity of 2.55. However, its CH_4 adsorption capacity is only 0.65 mmol g^{-1}.[106] A theoretical study using silicalite-I as the adsorbent for the concentration of CH_4 from low concentration CH_4/N_2 mixtures by a concentration thermal swing adsorption (CTSA) process has been reported by Delgado *et al.*[107] It would be interesting to see similar simulation work for VAM concentration with silicalite-I as the adsorbent for PSA processes.

The disadvantages of zeolites as sorbents for methane adsorption include low surface area, low CH_4 adsorption capacities and hydrophilic surface. As mentioned above, an adsorbent with high surface area associated with optimal pore size is the key prerequisite for methane adsorption, but the surface area of zeolites is generally low compared to porous carbon materials, which results in a low CH_4 adsorption capacity. In addition, the hydrophilic surface of zeolites will reduce the adsorption capacity in the presence of moisture (given the high relative humidity in ventilation air methane). Furthermore, zeolites with polar surfaces that possess high electric-field gradients have stronger interaction with CO_2 than with the non-polar CH_4 and N_2 molecules.[113] As can be observed from Table 2, most zeolites have a tendency to adsorb CO_2 over CH_4. The advantages of zeolites as the adsorbents are the low cost and mature synthesis technology of zeolites compared to MOFs. A new synthesis strategy that combines the advantages of zeolites (low cost and mature synthesis technology) and MOFs (high CH_4/N_2 selectivity), avoiding the complexity and high costs of synthesis processes of MOFs, is highly preferred to generate zeolites with both high CH_4/N_2 selectivity and high CH_4 adsorption capacity.

3.2. Porous carbon materials

Porous carbon materials, including high surface area activated carbons (ACs),[114,115] activated carbon fibers (ACFs),[92,116] and

Table 2 Textural properties, CH_4 adsorption capacity, CH_4/N_2 equilibrium selectivity and CO_2/CH_4 equilibrium selectivity of zeolites at 298 K and 100 kPa unless otherwise specified

Zeolites	BET surface area ($m^2\ g^{-1}$)	Pore volume ($cm^3\ g^{-1}$)	CH_4 uptake (mmol g^{-1})	Equilibrium selectivity CH_4/N_2	Equilibrium selectivity CO_2/CH_4	Ref.
Silicalite-I	439	0.19	0.65	3.60[a]	2.55[a]	106
Silicalite-I-H	323	0.137	0.67	3.9[a]	5.63[a]	108
Silicalite-I-M	342	0.130	0.67	3.9[a]	5.83[a]	108
K-KFI	430.4[b]	0.10[b]	0.78	8.5	35	105
Na-KFI	556.2[b]	0.15[b]	0.79	4.1	92	105
Li-KFI	550.6[b]	0.14[b]	0.71	3.0	80	105
Ca-KFI	333.5[b]	0.07[b]	0.72	3.0	19	105
K-CHA	278.5[b]	0.07[b]	0.85	14.5	24	105
Na-CHA	594.8[b]	0.16[b]	1.35	4.3	42	105
Li-CHA	638.0[b]	0.17[b]	1.47	4.7	32	105
5A	—	—	0.81	0.94[c]	256.47[c]	58
5A	—	—	0.69[f]	1.96[f]	—	103
13X	—	—	0.59	2.36[e]	14.9[e]	50
Linde 4A	—	0.108	0.95[g]	3.4[g]	6.5[g]	109
H-ZSM-5	—	—	0.71[h]	3.28[d,h]	6.11[d,h]	110
H-clinoptilolite	—	—	0.93	3.91[e,i]	—	111
K/Na (50 : 50)-clinoptilolite	—	—	1.05	3.27[e,i]	—	111
Zeolite X/AC composite	802	0.64	0.77	3.4[j]	—	112

[a] Calculated from the IAST model and values in brackets are the gas mixture ratio used for the calculation. [b] Measured by CO_2 adsorption at 273 K. [c] Calculated from Henry's selectivity. [d] Obtained at 303 K. [e] Calculated from Langmuir equation parameters. [f] Obtained at 305 K. [g] Obtained at 302 K. [h] Obtained at 313 K. [i] Obtained at 295 K. [j] Calculated from the ratio of adsorption amounts at 273 K.

carbon molecular sieves (CMSs),[117,118] have been extensively studied as the adsorbents in adsorption based processes for low concentration CH_4 recovery from unconventional natural gases[115,119,120] and VAM enrichment.[7,77,84–86] Table 3 summarizes the textural properties, CH_4 adsorption capacity, CH_4/N_2 selectivity and CO_2/CH_4 selectivity of porous carbon materials under ambient conditions unless otherwise specified.

3.2.1. Activated carbons (ACs). Due to their advantages, such as high CH_4 adsorption capacity, CH_4/N_2 selectivity, easy scale up and low price, ACs are the most studied carbon materials for CH_4 separation from CH_4 and N_2 gas mixtures. Much attention has been devoted to the investigation of the effect of the textural properties of ACs on the CH_4 adsorption capacity and the CH_4/N_2 selectivity. Optimal pore sizes of 0.7–0.9 nm,[121] 0.758–0.776 nm,[119] 0.7–1.3 nm,[122] 0.5–0.8 nm (ref. 120) and 0.55–0.85 nm (ref. 123) for high CH_4/N_2 selectivity have been suggested.

In addition, heteroatom-doped (N or S) porous carbons have also been extensively studied, and some N-doped carbons show very high CH_4/N_2 selectivity up to 8.6 for a 50 : 50 mixture.[64,124–126] Most of the reported N-doped porous carbons showed CH_4/N_2 selectivity lower than CO_2/CH_4 selectivity. However, N-doped AC with a high N content (>10 wt%) reported by Yao *et al.* showed a high CH_4 adsorption capacity of up to 1.47 mmol g^{-1} at 298 K and 100 kPa and high CH_4/N_2 selectivity up to 8.6, which was attributed to the unusually high N content as well as the suitably narrow ultramicropore size distribution.[64] In addition, it is worth pointing out that Li *et al.* reported that a N-doped AC (14.48 wt% N content) derived from waste wool showed a high CH_4/N_2 selectivity of 7.6 for a 50 : 50 mixture and 13.7 for a 5 : 95 mixture with a decent CH_4 adsorption of 1.01 mmol g^{-1}.[63]

Apart from the textural properties and N-doping, the surface chemistry properties of the porous carbons have also been found to be important for the gas separation performance.[127,128] For example, Tang *et al.* prepared binderless particle rice-based carbon materials (PRCs) with narrow micropore distribution by carbonization of rice followed by CO_2 activation, which showed a high CH_4 uptake of 1.12 mmol g^{-1} and a CH_4/N_2 selectivity of 5.7 at 298 K and 100 kPa.[128] Simulation calculations showed that the surface carboxyl groups played an important role in the improvement of the CH_4/N_2 selectivity. Fixed-bed experiments demonstrated that this carbon material can greatly separate CH_4/N_2 mixtures under ambient conditions.

3.2.2. Carbon molecular sieves (CMSs). Carbon molecular sieves (CMSs) are activated carbons with a relatively narrow micropore size distribution. As mentioned earlier, gas separation can be achieved by different equilibrium capacities (equilibrium separation) or by differences in the transport rate (kinetic separation). CMSs have been demonstrated to be able to separate CH_4 and N_2 by kinetic separation.[59,129,130] For example, Zhang *et al.* prepared a CMS by deposition and carbonization of benzene on activated carbon.[130] A CH_4 adsorption capacity of 1.33 mmol g^{-1}, an equilibrium CH_4/N_2 selectivity of 4.74 and a very high N_2/CH_4 kinetic selectivity of 35.26 were achieved. PSA results demonstrated a better performance in the separation of feed mixtures with a low concentration of CH_4.

3.2.3. Activated carbon fibers (ACFs). ACFs have a long history for gas separation and purification[92,116] and have fast intraparticle adsorption kinetics compared with pelletized or

Table 3 Textural properties, CH_4 adsorption capacity, CH_4/N_2 equilibrium selectivity and CO_2/CH_4 equilibrium selectivity of porous carbons at 298 K and 100 kPa unless otherwise specified

Carbon materials	BET surface area ($m^2\ g^{-1}$)	Pore volume ($cm^3\ g^{-1}$)	CH_4 uptake (mmol g^{-1})	Equilibrium selectivity CH_4/N_2	Equilibrium selectivity CO_2/CH_4	Ref.
AC[a] (from coconut shell)	329	0.145	—	6.18[c] (50 : 50)	—	84 and 85
ACF composites[a]	577	0.135[d]	—	**5.9**[e]/4.2[f]	3.29[f]	77
AC (GCTAC)	700	—	1.21	9.8[c] (2.5 : 97.5)	—	67
BPL AC	—	—	—	**4.5**[e]	2.5[e]	31
AC (CGUC-1-6)	624	0.267	1.01	5.9[c] (50 : 50)	16.9[c] (40 : 60)	134
AC (CGUC-1-8)	1071	0.439	1.34	5.0[c] (50 : 50)	9.4[c] (40 : 60)	134
AC (PRCs)	776	—	1.12	5.7[c] (15 : 85)	—	128
AC beads	1457	0.57	1.06	5.5[c,g] (50 : 50)	3.6[c,g] (50 : 50)	135
Granular AC	1227	0.505	1.59	3.2[g]	—	136
AC (SCs)	914	0.35	1.86	5.7[c] (50 : 50)	—	137
AC[b] (N-WAPC)	862	0.5	1.01	**7.62**[c] (50 : 50) **11.76**[c] (15 : 85) **13.71**[c] (5 : 95)	3.19[c] (50 : 50) 5.98[c] (15 : 85) 8.66[c] (5 : 95)	63
AC[b] (ClCTF-1-650)	974	0.37	1.47	**8.6**[c] (50 : 50)	8.1[c] (1 : 99)	64
AC[b] (ClCTF-1-550)	986	0.37	1.27	**8.1**[c] (50 : 50)	7.8[c] (1 : 99)	64
AC[b] (NAPC-2-6)	1247	0.69	1.3	4.1[c] (50 : 50)	10.1[c] (50 : 50)	124
AC[b] (OTSS-1-550)	778	0.31	1.49	5.22[c] (50 : 50)	8.15[c] (10 : 90)	138
AC[b] (SNMC-1-600)	1021	0.43	1.45	5.1[c] (50 : 50)	6.9[c] (40 : 60)	139
AC[b] (SNMC-2-600)	1884	0.78	1.57	4.2[c] (50 : 50)	4.3[c] (40 : 60)	139
AC[b] (SNMC-3-600)	3049	1.4	1.17	**3.6**[c] (50 : 50)	3.2[c] (40 : 60)	139
AC[b] (ACSs-N)	697	0.46	1.30	3.76[c]	7.49[c]	125
S-doped AC (CSK-7)	1324	0.81	1.23	2.92[c]	2.3[c]	126
CMS (1023)	389	0.182[d]	1.33	4.74[h]	—	130
Mesoporous carbon	599	0.66	1.05	5.8[e]	—	133
Mesoporous carbon (sOMC)	2255	2.17	0.90	**3.7**[c] (10 : 90)	2.8[c] (10 : 90)	132
Carbon composite (MNS-derived)	—	—	1.48	6.3[e]/10.4[i]	—	65
Carbon nanoplates (PCNPs)	690	—	1.17	10[c] (30 : 70)	—	66

[a] Carbon has been studied for VAM enrichment. [b] N-doped carbon. [c] Calculated from the IAST model and values in brackets are the gas mixture ratio used for the calculation. [d] Micropore volume. [e] Calculated from Henry's law constants. [f] Calculated from the initial slopes of adsorption isotherms at very low pressures. [g] Calculated at 303 K. [h] Calculated from Langmuir equation parameters. [i] Calculated from the initial slopes of adsorption isotherms at relevant pressures (CH_4 0.69 kPa and N_2 79.99 kPa).

granular ACs.[131] Honeycomb monolithic carbon fiber composites have been extensively studied as an adsorbent for the enrichment of VAM *via* a PSA process by Bae *et al.* They exhibited a CH_4/N_2 selectivity of 4.2 and 5.9 at 298 K obtained from the initial slopes of adsorption isotherms at very low pressures and from Henry's law constants, respectively, and have been applied in a prototype VAM enrichment unit.[7,77,86] It is important to develop other ACFs to improve the VAM enrichment performance.

3.2.4. Other carbon materials. Other carbon materials studied for CH_4/N_2 gas mixture separation include mesoporous carbon, carbon composites, carbon nanoplates, *etc.*[65,66,132,133] For example, Bae *et al.* reported new carbon composites which showed a CH_4/N_2 selectivity of about 10.4 calculated at each relevant partial pressure CH_4 0.69 kPa (0.66 vol%) and N_2 79.99 kPa (78.95 vol%) 79.99 kPa or 6.5 calculated at very low pressures.[65] Very recently, Xu *et al.* reported self-pillared ultramicroporous carbon nanoplates (PCNPs) with a CH_4/N_2 selectivity of 10 at 100 kPa and 298 K for a $30CH_4 : 70N_2$ mixture.[66] Further studies on the CO_2/CH_4 selectivity of these carbon nanoplates and their performance of VAM enrichment with SPA processes are highly needed.

As shown in Table 3, a lot of carbon materials with high CH_4 adsorption capacity and high CH_4/N_2 selectivity have been reported recently. So far the highest CH_4 adsorption capacity of 1.86 mmol g^{-1} with a CH_4/N_2 selectivity of 5.7 (for a 50 : 50 gas mixture) has been reported by Du *et al.*[137] and the highest CH_4/N_2 selectivity of 13.7 (for a 5 : 95 mixture) with a CH_4 adsorption capacity of 0.5 mmol g^{-1} has been reported by Li *et al.*[63] It is noteworthy that some of these ACs show CH_4/N_2 selectivity higher than the CO_2/CH_4 selectivity.[31,63,64,132,139] Given that ventilation air usually contains CO_2, it is highly desirable to study the VAM enrichment with SPA processes using these adsorbents. In addition, those carbon materials without available data on CO_2/CH_4 selectivity but with high CH_4 adsorption capacity and high CH_4/N_2 selectivity are potentially attractive too for VAM enrichment studies.[65–67,128,130]

Although porous carbon materials are generally hydrophobic, both experimental and theoretical studies show that microporous carbons can adsorb a large amount of water vapor.[140–142] Different from non-polar fluids, the adsorption mechanism of water in the micropores of carbon is determined by the balance between fluid–solid and fluid–fluid interactions, and it has been observed that the adsorption of water occurs *via* cluster formation.[142] It has also been demonstrated that the presence of water vapor adversely affects the adsorption capacity of microporous carbon and limits its effectiveness as an adsorbent material in humid environments.[140] Considering

the high relative humidity of ventilation air, it is important to study the effect of humidity on the adsorption capacities and selectivity of adsorbents in humid environments. In this respect, the adsorbent (carbon fiber composites) used in the site study for VAM enrichment by Bae *et al.* shows that the presence of moisture in ventilation air has no effect on CH_4 capture.[7] It is important to investigate the effect of water vapor on the adsorption performance of other porous carbon materials (with high CH_4 adsorption capacity and high CH_4/N_2 selectivity) that are potentially useful for VAM enrichment.

Compared to zeolites and MOFs, the downside of porous carbon materials would be the less control over the pore size distribution. However, porous carbon materials possess the advantages including high CH_4 adsorption capacity, high CH_4/N_2 selectivity, hydrophobicity, excellent chemical stability, low cost and ease of production. So far porous carbon materials have been the only adsorbents that have been used for site studies, demonstrating their potential in practical VAM enrichment.[7,84]

3.3. MOFs

MOFs, formed by coordination bonds between metal clusters and organic linkers, have great potential for gas adsorption and separation because of their high surface areas, tunable pore sizes, and versatile chemistry. Some MOFs have been investigated by molecular simulation studies, while plenty of MOFs have been experimentally studied for CH_4 separation from a CH_4/N_2 gas mixture. Table 4 summarizes the textural properties, CH_4 adsorption capacity, CH_4/N_2 selectivity and CO_2/CH_4 selectivity of MOFs at 100 kPa and 298 K unless otherwise specified.

Liu *et al.* carried out molecular simulation studies on the separation of CH_4/N_2 mixtures by using MOFs including Cu-BTC, MIL-47 (V), IRMOF-1, IRMOF-12, IRMOF-14, IRMOF-11, and IRMOF-13,[143] and ZIFs including ZIF-68 and ZIF-69.[144] The highest CH_4/N_2 selectivity of 4.7 was achieved for MIL-47 (V).[143] Peng *et al.* studied the adsorption and separation of CH_4/N_2 and CO_2/CH_4 of UMCM-1 and UMCM-2 using a hybrid method of computer simulation and adsorption theory.[145] A CH_4/N_2 selectivity of 2 was achieved for both MOF materials, which was insensitive to the pressure.

As listed in Table 4, for those frequently studied MOFs, so far the highest CH_4/N_2 selectivity of 12.5 has been reported by Li *et al.*[69] for an ultramicroporous squarate-based MOF, $[Co_3(C_4O_4)_2(OH)_2]$ ($C_4O_4^{2-}$ = squarate); however, the CH_4 adsorption capacity is low (0.40 mmol g^{-1}). In addition, a number of MOFs with very high CH_4/N_2 selectivity (6–12.5) have been reported in recent years,[38,40,68–71,146–152] with some of them also showing decent or extremely high CH_4 adsorption capacity (up to 2.9 mmol g^{-1}), making them very promising candidates for VAM or low grade CH_4 enrichment. Further studies on VAM enrichment using these MOFs with high CH_4/N_2 selectivity and decent or high CH_4 adsorption capacity are very much demanded.

The high CH_4/N_2 selectivity of those MOFs has been ascribed to the properties of the MOFs under study, including the uniform ultra-micropores and optimal polarizability,[39,40] or the suitable SOD cage size (0.84 nm) acting as a strong adsorption potential,[148] or the optimal coupling of the polarizability and structure of the MOF framework,[153] or strong interactions between CH_4 molecules and their coordinatively unsaturated metal sites,[68,151] or an increased number of polar sites,[38] *etc.* For example, it is known that coordinatively unsaturated metal centers can bind CH_4 significantly.[151] Niu *et al.* reported a CH_4 nano-trap that features oppositely adjacent open metal sites and dense alkyl groups in a MOF, ATC-Cu.[68] As illustrated in Fig. 7, when two opposite coordinatively unsaturated metal centers are adjacent to each other, a nano-trap for CH_4 can be generated based on the cooperative coulombic interaction between the CH_4 molecules and the two metal centers. This

Table 4 Textural properties, CH_4 adsorption capacity, CH_4/N_2 equilibrium selectivity and CO_2/CH_4 equilibrium selectivity of MOFs at 298 K and 100 kPa unless otherwise specified

Carbon materials	BET surface area (m^2 g^{-1})	Pore volume (cm^3 g^{-1})	CH_4 uptake (mmol g^{-1})	Selectivity CH_4/N_2	Selectivity CO_2/CH_4	Ref.
$[Co_3(C_4O_4)_2(OH)_2]$	76	—	0.40	**12.5**[a] (50 : 50)	—	69
Cu-MOF $[Cu(hfipbb)(H_2hfipbb)_{0.5}]$	105	—	0.46	6.9[b]	3.1[b]	146
Cu-MOF	110	—	0.63	**11.18**[e]	—	70
$[Ni_3(HCOO)_6]$	293	0.097[c]	0.82	6.18[d]	—	40
Ni(DOBDC)	1018	0.49	1.90	3.80[a] (50 : 50)	30[a] (50 : 50)	151
3D Ni-MOF	1168	0.807	1.76	7.0	—	152
$[Cu(INA)_2]$	252	0.12	0.80	8.34[d]	—	147
Cu(Me-4py-trz-ia)	1473	0.586	1.12	4.2[d]	—	156
ATC-Cu	600	0.23	**2.90**	**9.7**[a] (50 : 50)	—	68
CAU-21-BPDC (Al based MOF)	523	0.38	0.99	**11.9**[a] (50 : 50)	—	38
Co(DOBDC)	1089	0.50	**1.95**	3.2[a] (50 : 50)	40[a] (50 : 50)	151
ZIF-94	597	—	1.5	7[a] (30 : 70) (50 : 50)	—	148
ROD-8 (Cd^{II}-MOF)	369	—	0.77	**9.1**[e] (50 : 50)	3.3[e] (50 : 50)	71
ACF@$[Ni_3(HCOO)_6]$	1053	0.453	1.10	6.22	—	149
Ni-MA-BPY	464	0.160[c]c	1.01	7.4	—	150

[a] Calculated from the IAST model and values in brackets are the gas mixture ratio used for the calculation. [b] Calculated from Langmuir equation parameters. [c] Micropore volume. [d] Calculated from Henry's law constants. [e] Calculated with the dual-site Langmuir model and values in brackets are the gas mixture ratio used for the calculation.

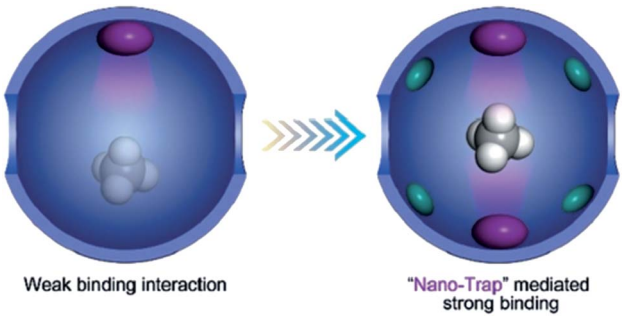

Fig. 7 The schematic comparison of a traditional CH_4 adsorbent and nano-trap. The purple and green ellipsoids represent coordinatively unsaturated metal centers and alkyl groups, respectively. Adapted with permission.[68] Copyright 2019, Wiley-VCH.

MOF showed a record-high CH_4 adsorption capacity of 2.90 mmol g^{-1} and a high CH_4/N_2 selectivity of 9.7 at 298 K and 100 kPa. Breakthrough experiments showed a complete separation of mixtures of $50CH_4 : 50N_2$ and $30CH_4 : 70N_2$ and good results for a $15CH_4 : 85N_2$ gas mixture.

Given that CH_4 has a greater polarizability than N_2, Lv *et al.* demonstrated a strategy to improve CH_4/N_2 selectivity by controlling the pore wall environment of two isomeric Al-based metal–organic frameworks (MOFs) with four highly symmetric polar sites for strengthened adsorption affinity toward CH_4 over N_2. At 298 K and 100 kPa, CAU-21-BPDC with four highly symmetric polar sites in the pore walls showed a CH_4 uptake capacity of 0.99 mmol g^{-1} and a CH_4/N_2 selectivity of 11.9, which was 2.4 times higher than that of the MOF without four highly symmetric polar sites.[38]

Apart from high CH_4/N_2 selectivity and high CH_4 adsorption capacity, considering that ventilation air is saturated with water, good water stability is also important for MOFs to be used as adsorbents for VAM separation/enrichment. It has been reported that one of the decisive factors in determining the water stability of MOFs is their metal clusters, with trinuclear chromium clusters more stable than copper paddlewheel clusters, which are more stable than basic zinc acetate clusters.[154] Other factors that affect the water stability including the strength of the bond between the metal oxide cluster and the bridging linker, the functionality of the ligand (hydrophilic or hydrophobic), the intrinsic textual properties, *etc.*, have been proposed.[155] Water stable MOFs with high CH_4/N_2 selectivity, such as $[Ni_3(HCOO)_6]$, three-dimensional Cu-MOF, squarate-based MOFs, Co-MA-BPY and Ni-MA-BPY, have been reported.[40,69,70,150] Moreover, due to the high relative humidity of ventilation air, apart from the water stability of MOFs, it is highly desirable to investigate the effect of water vapor on the adsorption performance of VAM for those promising MOF candidates with high CH_4 adsorption capacity and high CH_4/N_2 selectivity.

In addition, it is worth mentioning that Liu *et al.* prepared a formate metal–organic framework and activated carbon fiber composite, ACF@$[Ni_3(HCOO)_6]$, with a CH_4/N_2 selectivity of 6.22 and a CH_4 adsorption capacity of 1.10 mmol g^{-1}.[149] This strategy could be adopted for the preparation of other carbon/MOF composites with desired CH_4/N_2 selectivity and CH_4 adsorption capacity for gas separation/enrichment.

For most of the MOFs with CO_2/CH_4 selectivity available listed in Table 4, their CH_4/N_2 selectivities are lower than their CO_2/CH_4 selectivities, except in a few cases. In particular, Cu-MOF $[Cu(hfipbb)(H_2hfipbb)_{0.5}]$ showed a CH_4/N_2 selectivity of 6.9, CO_2/CH_4 selectivity of 3.1, and adsorption capacity of 0.46 mmol g^{-1},[146] and ROD-8 (Cd^{II}-MOF) showed a CH_4/N_2 selectivity of 9.1, CO_2/CH_4 selectivity of 3.3 and adsorption capacity of 0.77 mmol g^{-1}.[71] Considering the presence of CO_2 in ventilation air, these MOFs with CH_4/N_2 selectivity higher than their CO_2/CH_4 selectivity are very promising candidates for VAM enrichment.

The disadvantages of MOFs lie in the complexity and high cost of synthesis processes. On the other hand, MOFs have more flexibility in tuning the pore size and surface properties to achieve adsorbents with desired properties (*e.g.*, high CH_4 adsorption capacity, high CH_4/N_2 selectivity, and water stability). Some MOFs (in Table 4) show the highest CH_4 adsorption capacity among the widely studied three types of adsorbents (zeolites, porous carbon materials and MOFs), making them promising candidates for VAM enrichment.

3.4. Combination of adsorbents

Given that zeolites have stronger adsorption for CO_2 than for CH_4 and N_2, while carbon molecular sieves (CMSs) can kinetically separate CH_4 from N_2, a combination of zeolites and CMSs in a PSA system has been employed to separate the ternary mixtures of $CH_4/CO_2/N_2$. For example, ACs, CMS, and zeolite 13X in a specially designed PSA has shown that CO_2, CH_4 and N_2 could apparently be enriched in the top, side and bottom product streams, respectively.[157] In addition, a layered pressure swing adsorption (LPSA) system based on the assumption that CO_2 would be almost completely adsorbed in 13X followed by kinetic separation of CH_4/N_2 in the CMS layer has been demonstrated to be able to enrich CH_4 from 60% to 86%.[35] The combination of different types of adsorbents in PSA processes for VAM enrichment could be a choice to simultaneously collect CH_4, CO_2 and N_2 separately, which could add value to the processes.

3.5. Summary of adsorption materials

In general, the limitation of zeolites as the adsorbent for CH_4 separation lies in the low CH_4/N_2 selectivity and low CH_4 adsorption capacity compared to porous carbons and MOFs, and the hydrophilic surface. A number of porous carbons and MOFs exhibiting both high CH_4/N_2 selectivity and high CH_4 adsorption capacity are very promising candidates for VAM enrichment, especially those with CH_4/N_2 selectivity higher than CO_2/CH_4 selectivity, and some MOFs show the highest CH_4 adsorption capacity among the widely studied three types of adsorbents. So far porous carbon materials have been the only sorbents that have been used in site studies for VAM ventilation. However, further studies on the VAM enrichment performance, regenerability, kinetics, compatibility and cost are highly desirable for their practical applications. Porous carbons have the advantages of excellent chemical stability, low cost and ease

of production, while MOFs have more flexibilities on the pore size, surface property, *etc.* New strategies to produce novel porous materials that combine the advantages of zeolites and MOFs or the advantages of carbon and MOFs could lead to promising adsorbents with desired properties for gas enrichment, such as high CH_4/N_2 selectivity, high CH_4 adsorption capacity, easy regenerability, good chemical stability, *etc.*

4. Conclusions and prospects

We have presented an overview on the technologies and materials for VAM enrichment with focus on adsorption-based processes (PSA and TSA). PSA processes have been the most studied and the most promising technology for VAM enrichment so far. A pilot-scale study with VPSA and a site trial with VTSA for VAM enrichment have been carried out, respectively. Further studies on the cost, efficiency, scalability *etc.* of these technologies are needed.

The adsorbents used in the adsorption processes (PSA and TSA) are one of the key factors for gas separation/enrichment performance. We have summarized materials that are potentially useful for VAM enrichment, including zeolites, porous carbon materials and MOFs with focus on those with high CH_4/N_2 selectivity and high CH_4 adsorption capacity and highlighted new synthesis strategies to achieve high CH_4 adsorption capacity and CH_4/N_2 equilibrium selectivity. In general, zeolites exhibit low CH_4/N_2 selectivity and low CH_4 adsorption capacity compared to porous carbons and MOFs. Several porous carbons and MOFs exhibiting both high CH_4/N_2 selectivity (up to 12.5) and high CH_4 adsorption capacity (up to 2.90 mmol g^{-1}) are very promising candidates for VAM enrichment,[38,63–71] especially those with CH_4/N_2 selectivity higher than CO_2/CH_4 selectivity. Making use of these adsorbents in PSA and/or TSA processes is likely to result in desirable VAM enrichment performance.

New synthesis strategies including the combination of the advantages of zeolites and MOFs, or the advantages of carbon and MOFs, heteroatom (N or S) doping, and surface property modification for porous carbons, the creation of coordinatively unsaturated metal centers for MOFs and the pore wall environment control of MOFs could lead to novel adsorbents with desirable properties such as high CH_4/N_2 selectivity, high CH_4 adsorption capacity, easy regenerability, good chemical stability, *etc.* for VAM enrichment.

This review will inspire further studies and advances for VAM enrichment to better mitigate and utilize VAM or other low grade CH_4, which will not only cut down on CH_4 emissions, but also provide extra economic benefits to the mining industry and ultimately contribute to the future low carbon economy.

Conflicts of interest

There are no conflicts to declare.

Acknowledgements

This work was supported by the EU RFCS [RFCS-2016-754077] and Leverhulme Trust [RPG-2018-320].

References

1 IPCC, *Global Warming Potential Values. Intergovernmental Panel on Climate Change*, http://ghgprotocol.org/sites/default/files/ghgp/Global-Warming-Potential-Values%20(Feb%2016%202016).pdf, 2016.
2 *Global Methane Emissions and Mitigation Opportunities, Global Methane Initiative*, https://www.globalmethane.org/documents/gmi-mitigation-factsheet.pdf, 2020.
3 N. Kholod, M. Evans, R. C. Pilcher, V. Roshchanka, F. Ruiz, M. Cote and R. Collings, *J. Cleaner Prod.*, 2020, **256**, 120489.
4 S. Su, H. W. Chen, P. Teakle and S. Xue, *J. Environ. Manage.*, 2008, **86**, 44–62.
5 R. Thiruvenkatachari, S. Su and X. X. Yu, *J. Hazard. Mater.*, 2009, **172**, 1505–1511.
6 I. Karakurt, G. Aydin and K. Aydiner, *Renewable Sustainable Energy Rev.*, 2011, **15**, 1042–1049.
7 J. S. Bae, S. Su, X. X. Yu, J. J. Yin, A. Villella, M. Jara and M. Loney, *Ind. Eng. Chem. Res.*, 2020, **59**, 15732–15741.
8 S. Su, A. Beath, H. Guo and C. Mallett, *Prog. Energy Combust. Sci.*, 2005, **31**, 123–170.
9 P. Hinde, I. Mitchell and M. Riddell, *Johnson Matthey Technol. Rev.*, 2016, **60**, 211–221.
10 J. J. Yin, S. Su, X. X. Yu, J. S. Bae, Y. G. Jin, A. Villella, M. Jara, M. Ashby, M. Cunnington and M. Loney, *Energy Fuels*, 2020, **34**, 9885–9893.
11 D. Ursueguía, P. Marín, E. Díaz and S. Ordóñez, *J. Nat. Gas Sci. Eng.*, 2021, **88**, 103808.
12 P. Marín, F. V. Díez and S. Ordóñez, *Chem. Eng. Process.*, 2019, **135**, 175–189.
13 X. Jiang, D. Mira and D. L. Cluff, *Prog. Energy Combust. Sci.*, 2018, **66**, 176–199.
14 R. I. Holmes, *Journal of Applied Engineering Sciences*, 2016, **6**, 41–50.
15 L. Hoglund-Isaksson, *Atmos. Chem. Phys.*, 2012, **12**, 9079–9096.
16 I. Karakurt, G. Aydin and K. Aydiner, *Renewable Energy*, 2012, **39**, 40–48.
17 R. O. Yusuf, Z. Z. Noor, A. H. Abba, M. A. Abu Hassan and M. F. M. Din, *Renewable Sustainable Energy Rev.*, 2012, **16**, 5059–5070.
18 C. Pratt and K. Tate, *Environ. Sci. Technol.*, 2018, **52**, 6084–6097.
19 M. R. Kulkarni and C. R. Sardesai, *J. Energy Eng.*, 2002, **128**, 1–12.
20 C. U. Linderstrøm-Lang, *Int. J. Heat Mass Transfer*, 1964, **7**, 1195–1206.
21 R. Manimaran, *Aust. J. Mech. Eng.*, 2020, **29**, 1816735.
22 S. Mohammadi and F. Farhadi, *Sep. Purif. Technol.*, 2014, **138**, 177–185.
23 J. Yun, Y. Kim and S. Yu, *Int. J. Heat Mass Transfer*, 2018, **126**, 353–361.
24 W. Wang, H. Wang, H. M. Li, D. Y. Li, H. B. Li and Z. H. Li, *Energies*, 2018, **11**, 428.
25 W. Wang, J. D. Ren, X. J. Li, H. B. Li, D. Y. Li, H. M. Li and Y. Song, *Sci. Rep.*, 2020, **10**, 7276.

26 T. P. Adamova, O. S. Subbotin, L. J. Chen and V. R. Belosludov, *J. Eng. Thermophys.*, 2013, **22**, 62–68.
27 J. W. Du, H. J. Li and L. G. Wang, *Ind. Eng. Chem. Res.*, 2014, **53**, 8182–8187.
28 J. W. Du, H. J. Li and L. G. Wang, *Chem. Eng. J.*, 2015, **273**, 75–81.
29 D. Saha, H. A. Grappe, A. Chakraborty and G. Orkoulas, *Chem. Rev.*, 2016, **116**, 11436–11499.
30 S. Sridhar, B. Smitha and T. M. Aminabhavi, *Sep. Purif. Rev.*, 2007, **36**, 113–174.
31 S. Sircar and T. C. Golden, *Sep. Sci. Technol.*, 2000, **35**, 667–687.
32 J. G. Jee, J. S. Lee and C. H. Lee, *Ind. Eng. Chem. Res.*, 2001, **40**, 3647–3658.
33 S. U. Nandanwar, D. R. Corbin and M. B. Shiflett, *Ind. Eng. Chem. Res.*, 2020, **59**, 13355–13369.
34 A. Olajossy, A. Gawdzik, Z. Budner and J. Dula, *Chem. Eng. Res. Des.*, 2003, **81**, 474–482.
35 S. Cavenati, C. A. Grande and A. E. Rodrigues, *Chem. Eng. Sci.*, 2006, **61**, 3893–3906.
36 T. E. Rufford, S. Smart, G. C. Y. Watson, B. F. Graham, J. Boxall, J. C. D. da Costa and E. F. May, *J. Pet. Sci. Eng.*, 2012, **94–95**, 123–154.
37 T. C. Golden and S. Sircar, *J. Colloid Interface Sci.*, 1994, **162**, 182–188.
38 D. F. Lv, Y. Wu, J. Y. Chen, Y. H. Tu, Y. N. Yuan, H. X. Wu, Y. W. Chen, B. Y. Liu, H. X. Xi, Z. Li and Q. B. Xia, *AIChE J.*, 2020, **66**, e16287.
39 X. Y. Ren, T. J. Sun, J. L. Hu and S. D. Wang, *Microporous Mesoporous Mater.*, 2014, **186**, 137–145.
40 Y. Guo, J. L. Hu, X. W. Liu, T. J. Sun, S. S. Zhao and S. D. Wang, *Chem. Eng. J.*, 2017, **327**, 564–572.
41 J. Kim, A. Maiti, L. C. Lin, J. K. Stolaroff, B. Smit and R. D. Aines, *Nat. Commun.*, 2013, **4**, 1694.
42 A. Eslamimanesh, A. H. Mohammadi, D. Richon, P. Naidoo and D. Ramjugernath, *J. Chem. Thermodyn.*, 2012, **46**, 62–71.
43 M. Arjmandi, A. Chapoy and B. Tohidi, *J. Chem. Eng. Data*, 2007, **52**, 2153–2158.
44 J. Z. Zhao, Y. S. Zhao and W. G. Liang, *Energy Technol.*, 2016, **4**, 864–869.
45 T. Suginaka, H. Sakamoto, K. Iino, Y. Sakakibara and R. Ohmura, *Fluid Phase Equilib.*, 2013, **344**, 108–111.
46 D. L. Zhong, Y. Ye, C. Yang, Y. Bian and K. Ding, *Ind. Eng. Chem. Res.*, 2012, **51**, 14806–14813.
47 J. Cai, C. G. Xu, Z. M. Xia, Z. Y. Chen and X. S. Li, *Appl. Energy*, 2017, **204**, 1526–1534.
48 T. Rodenas, M. van Dalen, E. Garcia-Perez, P. Serra-Crespo, B. Zornoza, F. Kapteijn and J. Gascon, *Adv. Funct. Mater.*, 2014, **24**, 249–256.
49 P. Marín, Z. Yang, Y. Xia and S. Ordóñez, *J. Nat. Gas Sci. Eng.*, 2020, **81**, 103420.
50 S. Cavenati, C. A. Grande and A. E. Rodrigues, *J. Chem. Eng. Data*, 2004, **49**, 1095–1101.
51 S. Cavenati, C. A. Grande and A. E. Rodrigues, *Sep. Sci. Technol.*, 2005, **40**, 2721–2743.
52 Q. Wu, L. Zhou, J. Q. Wu and Y. P. Zhou, *J. Chem. Eng. Data*, 2005, **50**, 635–642.
53 G. Watson, E. F. May, B. F. Graham, M. A. Trebble, R. D. Trengove and K. I. Chan, *J. Chem. Eng. Data*, 2009, **54**, 2701–2707.
54 Z. Huang, L. Xu, J. H. Li, G. M. Guo and Y. Wang, *J. Chem. Eng. Data*, 2010, **55**, 2123–2127.
55 C. A. Grande, Advances in Pressure Swing Adsorption for Gas Separation, *ISRN Chem. Eng.*, 2012, 982934.
56 M. B. Kim, Y. S. Bae, D. K. Choi and C. H. Lee, *Ind. Eng. Chem. Res.*, 2006, **45**, 5050–5058.
57 J. F. Yang, R. Krishna, J. M. Li and J. P. Li, *Microporous Mesoporous Mater.*, 2014, **184**, 21–27.
58 D. Saha, Z. B. Bao, F. Jia and S. G. Deng, *Environ. Sci. Technol.*, 2010, **44**, 1820–1826.
59 Y. Yang, A. M. Ribeiro, P. Li, J. G. Yu and A. E. Rodrigues, *Ind. Eng. Chem. Res.*, 2014, **53**, 16840–16850.
60 T. E. S. Rufford, G. C. Y. Watson, B. F. Graham, J. Boxall, J. C. Diniz da Costa and E. F. Maya, *J. Pet. Sci. Eng.*, 2012, **94–95**, 32.
61 US EPA, *Assessment of the worldwide market potential for oxidizing coal mine ventilation air methane*, United States Environmental Protection Agency, EPA 430-R-03-002, July 2003.
62 P. Franklin, *US Environmental Protection Agency VAM Vendor's Workshop Summary*, Washington DC, 2nd and 3rd June 2004.
63 Y. Li, R. Xu, B. B. Wang, J. P. Wei, L. Y. Wang, M. Q. Shen and J. Yang, *Nanomaterials*, 2019, **9**, 266.
64 K. X. Yao, Y. L. Chen, Y. Lu, Y. F. Zhao and Y. Ding, *Carbon*, 2017, **122**, 258–265.
65 J. S. Bae, Y. G. Jin, C. Huynh and S. Su, *J. Environ. Manage.*, 2018, **217**, 373–380.
66 S. Xu, W.-C. Li, C.-T. Wang, L. Tang, G.-P. Hao and A.-H. Lu, *Angew. Chem., Int. Ed.*, 2020, **60**, 6339–6343.
67 G. P. Hu, Q. H. Zhao, L. F. Tao, P. Xiao, P. A. Webley and K. G. Li, *Chem. Eng. Sci.*, 2021, **229**, 116152.
68 Z. Niu, X. L. Cui, T. Pham, P. C. Lan, H. B. Xing, K. A. Forrest, L. Wojtas, B. Space and S. Q. Ma, *Angew. Chem., Int. Ed.*, 2019, **58**, 10138–10141.
69 L. Y. Li, L. F. Yang, J. W. Wang, Z. G. Zhang, Q. W. Yang, Y. W. Yang, Q. L. Ren and Z. B. Bao, *AIChE J.*, 2018, **64**, 3681–3689.
70 M. Chang, Y. J. Zhao, Q. Y. Yang and D. H. Liu, *ACS Omega*, 2019, **4**, 14511–14516.
71 R. J. Li, M. Li, X. P. Zhou, S. W. Ng, M. O'Keeffe and D. Li, *CrystEngComm*, 2014, **16**, 6291–6295.
72 M. Tagliabue, D. Farrusseng, S. Valencia, S. Aguado, U. Ravon, C. Rizzo, A. Corma and C. Mirodatos, *Chem. Eng. J.*, 2009, **155**, 553–566.
73 D. Tondeur and P. C. Wankat, *Sep. Purif. Methods*, 1985, **14**, 157–212.
74 S. Cavenati, C. A. Grande and A. E. Rodrigues, *Energy Fuels*, 2006, **20**, 2648–2659.
75 C. A. Grande and A. E. Rodrigues, *Ind. Eng. Chem. Res.*, 2007, **46**, 4595–4605.
76 G. S. Duarte, B. Schurer, C. Voss and D. Bathen, *ChemBioEng Rev.*, 2017, **4**, 277–288.

77 J. S. Bae, S. Su and X. X. Yu, *Environ. Sci. Technol.*, 2014, **48**, 6043–6049.
78 Y. Zhou, Q. Fu, Y. H. Shen, W. N. Sun, D. H. Zhang, D. D. Li and H. Y. Yan, *Energy Fuels*, 2016, **30**, 1496–1509.
79 Y. L. Li, Y. S. Liu and X. Yang, *Sep. Sci. Technol.*, 2013, **48**, 1201–1210.
80 D. L. Qu, Y. Yang, Z. L. Qian, P. Li, J. G. Yu, A. M. Ribeiro and A. E. Rodrigues, *Chem. Eng. J.*, 2020, **380**, 122509.
81 Y. L. Li, Y. Meng, Y. S. Liu, X. Yang and C. Z. Zhang, *Adv. Mechan. Design, Parts 1–3*, ed. W. Z. Chen, P. Dai, Y. L. Chen, Q. T. Wang and Z. Jiang, 2012, 479–481, pp. 648–653.
82 Y. L. Li, C. Z. Zhang, Y. S. Liu, X. Yang and Y. Meng, *Adv. Mechan. Design, Parts 1–3*, ed. W. Z. Chen, P. Dai, Y. L. Chen, Q. T. Wang and Z. Jiang, 2012, 479–481, pp. 260–265.
83 X. Yang, Y. S. Liu and Y. L. Li, *Chem. Eng. Mater. Properties, Parts 1 and 2*, ed. H. M. Zhang and B. Wu, 2012, 391–392, pp. 1253–1258.
84 X. Yang, Y. S. Liu, Z. Y. Li, C. Z. Zhang and Y. Xing, *Energies*, 2018, **11**, 1030.
85 S. B. Ouyang, S. P. Xu, N. Song and S. L. Jiao, *Fuel*, 2013, **113**, 420–425.
86 J. S. Bae, S. Su and X. X. Yu, *Ind. Eng. Chem. Res.*, 2019, **58**, 21700–21707.
87 Y. S. Liu, X. Yang, Y. L. Li, H. J. Yang, C. Z. Zhang and Y. Meng, *Energy Educ. Sci. Technol., Part A*, 2012, **29**, 217–226.
88 Y. Yang, Y. J. Wu, H. Q. Liu, A. M. Ribeiro, P. Li, J. G. Yu and A. E. Rodrigues, *Chem. Eng. Sci.*, 2016, **149**, 215–228.
89 C. M. Liu, Y. P. Zhou, Y. Sun, W. Su and L. Zhou, *AIChE J.*, 2011, **57**, 645–654.
90 V. C. Menon and S. Komarneni, *J. Porous Mater.*, 1998, **5**, 43–58.
91 K. F. Loughlin, M. M. Hassan, A. I. Fatehi and M. Zahur, *Gas Sep. Purif.*, 1993, **7**(4), 264–273.
92 G. Q. Lu and M. RostamAbadi, *Gas Sep. Purif.*, 1996, **10**, 89–90.
93 J. W. Yoon, H. Chang, S. J. Lee, Y. K. Hwang, D. Y. Hong, S. K. Lee, J. S. Lee, S. Jang, T. U. Yoon, K. Kwac, Y. Jung, R. S. Pillai, F. Faucher, A. Vimont, M. Daturi, G. Ferey, C. Serre, G. Maurin, Y. S. Bae and J. S. Chang, *Nat. Mater.*, 2017, **16**, 526–531.
94 D. E. Jaramillo, D. A. Reed, H. Z. H. Jiang, J. Oktawiec, M. W. Mara, A. C. Forse, D. J. Lussier, R. A. Murphy, M. Cunningham, V. Colombo, D. K. Shuh, J. A. Reimer and J. R. Long, *Nat. Mater.*, 2020, **19**, 517–521.
95 J. H. Zhao, S. H. Mousavi, G. K. Xiao, A. H. Mokarizadeh, T. Moore, K. F. Chen, Q. F. Gu, R. Singh, A. Zavabeti, J. Z. Liu, P. A. Webley and G. K. Li, *J. Am. Chem. Soc.*, 2021, **143**, 15195–15204.
96 F. F. Zhang, K. J. Li, J. Chen, X. R. Zhang, K. B. Li, H. Shang, L. Ma, W. J. Guo, X. L. Wu, J. F. Yang and J. P. Li, *Sep. Purif. Technol.*, 2022, **281**, 119951.
97 A. Policicchio, R. Filosa, S. Abate, G. Desiderio and E. Colavita, *J. Porous Mater.*, 2017, **24**, 905–922.
98 J. Alcaniz-Monge, D. Lozano-Castello, D. Cazorla-Amoros and A. Linares-Solano, *Microporous Mesoporous Mater.*, 2009, **124**, 110–116.
99 C. Guan, F. B. Su, X. S. Zhao and K. Wang, *Sep. Purif. Technol.*, 2008, **64**, 124–126.
100 D. Lozano-Castello, D. Cazorla-Amoros, A. Linares-Solano and D. F. Quinn, *Carbon*, 2002, **40**, 989–1002.
101 N. Kosinov, J. Gascon, F. Kapteijn and E. J. M. Hensen, *J. Membr. Sci.*, 2016, **499**, 65–79.
102 Y. Q. Wu, D. H. Yuan, D. W. He, J. C. Xing, S. Zeng, S. T. Xu, Y. P. Xu and Z. M. Liu, *Angew. Chem., Int. Ed.*, 2019, **58**, 10241–10244.
103 J. A. C. Silva, A. Ferreira, P. A. P. Mendes, A. F. Cunha, K. Gleichmann and A. E. Rodrigues, *Ind. Eng. Chem. Res.*, 2015, **54**, 6390–6399.
104 G. M. Nam, B. M. Jeong, S. H. Kang, B. K. Lee and D. K. Choi, *J. Chem. Eng. Data*, 2005, **50**, 72–76.
105 J. F. Yang, Q. Zhao, H. Xu, L. B. Li, J. X. Dong and J. P. Li, *J. Chem. Eng. Data*, 2012, **57**, 3701–3709.
106 J. F. Yang, J. M. Li, W. Wang, L. B. Li and J. P. Li, *Ind. Eng. Chem. Res.*, 2013, **52**, 17856–17864.
107 J. A. Delgado, V. I. Agueda, J. Garcia and S. Alvarez-Torrellas, *Sep. Purif. Technol.*, 2019, **209**, 550–559.
108 J. F. Yang, N. Yuan, M. Xu, J. Q. Liu, J. P. Li and S. G. Deng, *Microporous Mesoporous Mater.*, 2018, **266**, 56–63.
109 N. K. Jensen, T. E. Rufford, G. Watson, D. K. Zhang, K. I. Chan and E. F. May, *J. Chem. Eng. Data*, 2012, **57**, 106–113.
110 P. J. E. Harlick and F. H. Tezel, *Sep. Sci. Technol.*, 2002, **37**, 33–60.
111 A. Jayaraman, A. J. Hernandez-Maldonado, R. T. Yang, D. Chinn, C. L. Munson and D. H. Mohr, *Chem. Eng. Sci.*, 2004, **59**, 2407–2417.
112 C. L. Xue, W. P. Cheng, W. M. Hao, J. H. Ma and R. F. Li, *J. Chem.*, 2019, **2019**, 2078360.
113 J. R. Li, R. J. Kuppler and H. C. Zhou, *Chem. Soc. Rev.*, 2009, **38**, 1477–1504.
114 I. Esteves, M. S. S. Lopes, P. M. C. Nunes and J. P. B. Mota, *Sep. Purif. Technol.*, 2008, **62**, 281–296.
115 T. L. Saleman, G. Li, T. E. Rufford, P. L. Stanwix, K. I. Chan, S. H. Huang and E. F. May, *Chem. Eng. J.*, 2015, **281**, 739–748.
116 G. M. Kimber, M. Jagtoyen, Y. Q. Fei and F. J. Derbyshire, *Gas Sep. Purif.*, 1996, **10**, 131–136.
117 S. Cavenati, C. A. Grande and A. E. Rodrigues, *Sep. Sci. Technol.*, 2005, **40**, 2721–2743.
118 A. Jayaraman, A. S. Chiao, J. Padin, R. T. Yang and C. L. Munson, *Sep. Sci. Technol.*, 2002, **37**, 2505–2528.
119 G. F. Zhao, P. Bai, H. M. Zhu, R. X. Yan, X. M. Liu and Z. F. Yan, *Asia-Pac. J. Chem. Eng.*, 2008, **3**, 284–291.
120 M. Gu, B. Zhang, Z. D. Qi, Z. J. Liu, S. Duan, X. D. Du and X. F. Xian, *Sep. Purif. Technol.*, 2015, **146**, 213–218.
121 P. Kluson, S. Scaife and N. Quirke, *Sep. Purif. Technol.*, 2000, **20**, 15–24.
122 C. M. Liu, Y. Y. Dang, Y. P. Zhou, J. Liu, Y. Sun, W. Su and L. Zhou, *Adsorption*, 2012, **18**, 321–325.
123 D. S. Yuan, Y. N. Zheng, Q. Z. Li, B. Q. Lin, G. Y. Zhang and J. F. Liu, *Powder Technol.*, 2018, **333**, 377–384.
124 J. Wang, P. X. Zhang, L. Liu, Y. Zhang, J. F. Yang, Z. L. Zeng and S. G. Deng, *Chem. Eng. J.*, 2018, **348**, 57–66.

125 J. Wang, R. Krishna, J. F. Yang, K. P. R. Dandamudi and S. G. Deng, *Mater. Today Commun.*, 2015, **4**, 156–165.
126 W. Su, L. Yao, M. Ran, Y. Sun, J. Liu and X. J. Wang, *J. Chem. Eng. Data*, 2018, **63**, 2914–2920.
127 H. Y. Pan, Y. Yi, Q. Lin, G. Y. Xiang, Y. Zhang and F. Liu, *J. Chem. Eng. Data*, 2016, **61**, 2120–2127.
128 R. L. Tang, Q. B. Dai, W. W. Liang, Y. Wu, X. Zhou, H. Y. Pan and Z. Li, *Chem. Eng. J.*, 2020, **384**, 123388.
129 S. Cavenati, C. A. Grande and A. E. Rodrigues, *Sep. Sci. Technol.*, 2005, **40**, 2721–2743.
130 J. H. Zhang, S. J. Qu, L. T. Li, P. Wang, X. F. Li, Y. F. Che and X. L. Li, *J. Chem. Eng. Data*, 2018, **63**, 1737–1744.
131 M. Suzuki, *Carbon*, 1994, **32**, 577–586.
132 B. Yuan, X. F. Wu, Y. X. Chen, J. H. Huang, H. M. Luo and S. G. Deng, *Environ. Sci. Technol.*, 2013, **47**, 5474–5480.
133 B. Yuan, X. F. Wu, Y. X. Chen, J. H. Huang, H. M. Luo and S. G. Deng, *J. Colloid Interface Sci.*, 2013, **394**, 445–450.
134 P. X. Zhang, J. Wang, W. Fan, Y. Zhong, Y. Zhang, Q. Deng, Z. L. Zeng and S. G. Deng, *Chem. Eng. J.*, 2019, **375**, 121931.
135 Y. J. Wu, Y. Yang, X. M. Kong, P. Li, J. G. Yu, A. M. Ribeiro and A. E. Rodrigues, *J. Chem. Eng. Data*, 2015, **60**, 2684–2693.
136 D. L. Qu, Y. Yang, K. Lu, L. Yang, P. Li, J. G. Yu, A. M. Ribeiro and A. E. Rodrigues, *Adsorption*, 2018, **24**, 357–369.
137 S. J. Du, Y. Wu, X. J. Wang, Q. B. Xia, J. Xiao, X. Zhou and Z. Li, *AIChE J.*, 2020, **66**, e16231.
138 Y. Zhang, L. Liu, P. X. Zhang, J. Wang, M. Xu, Q. Deng, Z. L. Zeng and S. G. Deng, *Chem. Eng. J.*, 2019, **355**, 309–319.
139 P. X. Zhang, Y. Zhong, J. Ding, J. Wang, M. Xu, Q. Deng, Z. L. Zeng and S. G. Deng, *Chem. Eng. J.*, 2019, **355**, 963–973.
140 B. P. Russell and M. D. LeVan, *Ind. Eng. Chem. Res.*, 1997, **36**, 2380–2389.
141 T. Ohba and K. Kaneko, *Langmuir*, 2011, **27**, 7609–7613.
142 J. Bahadur, C. I. Contescu, D. K. Rai, N. C. Gallego and Y. B. Melnichenko, *Carbon*, 2017, **111**, 681–688.
143 B. Liu and B. Smit, *Langmuir*, 2009, **25**, 5918–5926.
144 B. Liu and B. Smit, *J. Phys. Chem. C*, 2010, **114**, 8515–8522.
145 X. Peng, X. Cheng and D. P. Cao, *J. Mater. Chem.*, 2011, **21**, 11259–11270.
146 X. F. Wu, B. Yuan, Z. B. Bao and S. G. Deng, *J. Colloid Interface Sci.*, 2014, **430**, 78–84.
147 J. L. Hu, T. J. Sun, X. W. Liu, Y. Guo and S. D. Wang, *RSC Adv.*, 2016, **6**, 64039–64046.
148 Q. Shi, J. Wang, H. Shang, H. H. Bai, Y. Zhao, J. F. Yang, J. X. Dong and J. P. Li, *Sep. Purif. Technol.*, 2020, **230**, 115850.
149 X. W. Liu, J. L. Hu, T. J. Sun, Y. Guo, T. D. Bennett, X. Y. Ren and S. D. Wang, *Chem.–Asian J.*, 2016, **11**, 3014–3017.
150 X. W. Liu, Y. M. Gu, T. J. Sun, Y. Guo, X. L. Wei, S. S. Zhao and S. D. Wang, *Ind. Eng. Chem. Res.*, 2019, **58**, 20392–20400.
151 L. B. Li, J. F. Yang, J. M. Li, Y. Chen and J. P. Li, *Microporous Mesoporous Mater.*, 2014, **198**, 236–246.
152 C. E. Kivi, B. S. Gelfand, H. Dureckova, H. T. K. Ho, C. Ma, G. K. H. Shimizu, T. K. Woo and D. T. Song, *Chem. Commun.*, 2018, **54**, 14104–14107.
153 J. L. Hu, T. J. Sun, X. Y. Ren and S. D. Wang, *Microporous Mesoporous Mater.*, 2015, **204**, 73–80.
154 K. A. Cychosz and A. J. Matzger, *Langmuir*, 2010, **26**, 17198–17202.
155 W. Zhang, Y. L. Hu, J. Ge, H. L. Jiang and S. H. Yu, *J. Am. Chem. Soc.*, 2014, **136**, 16978–16981.
156 J. Mollmer, M. Lange, A. Moller, C. Patzschke, K. Stein, D. Lassig, J. Lincke, R. Glaser, H. Krautscheid and R. Staudt, *J. Mater. Chem.*, 2012, **22**, 10274–10286.
157 F. Dong, H. M. Lou, A. Kodama, M. Goto and T. Hirose, *Sep. Purif. Technol.*, 1999, **16**, 159–166.